Regulation of neuron-specific gene transcription by stress hormone signalling requires synaptic activity in zebrafish

Helen Eachus[1*#], Dheemanth Subramanya[1*], Harriet E. Jackson[1##], Guannyu Wang[1], Kieran Berntsen[1], John-Paul Ashton[1], Umberto Esposito[2], Fayaz Seifuddin[3], Mehdi Pirooznia[3], Eran Elhaik[2], Nils Krone[4], Richard A. Baines[5], Marysia Placzek[1], Vincent T. Cunliffe[1**]

* These authors contributed equally to this work

** Corresponding author, ORCID 0000-0001-7483-7610

1: Department of Biomedical Science, University of Sheffield, Firth Court, Western Bank, Sheffield S10 2TN, UK

2: Department of Animal and Plant Sciences, University of Sheffield, Alfred Denny Building, Western Bank, Sheffield S10 2TN, UK

3: Bioinformatics and Computational Biology, National Heart, Lung and Blood Institute, National Institutes of Health, Building 12, 12 South Drive, Bethesda, MD 20892, USA

4: Department of Oncology and Metabolism, Medical School, University of Sheffield, Beech Hill Road, Sheffield S10 2RX, UK

5: Division of Neuroscience and Experimental Psychology, School of Biological Sciences, Faculty of Biology, Medicine and Health, University of Manchester, Manchester Academic Health Science Centre, Manchester, M13 9PL, UK

Current Address: German Resilience Center, University Medical Center, Johannes Gutenberg University Mainz, Duesbergweg 6, 55128 Mainz, Germany

Current Address: Department of Genetics, St Mary's Hospital, Oxford Road, Manchester M13 9WL, UK

Abstract

The Glucocorticoid Receptor (GR) co-ordinates metabolic and behavioural responses to stressors. We hypothesised that GR influences behaviour by modulating specific epigenetic and transcriptional processes in the brain. Using the zebrafish as a model organism, the brain methylomes of wild-type and *gr*^{s357} mutant adults were analysed and GR-sensitive, differentially methylated regions (GR-DMRs) were identified. Two genes with GR-DMRs exhibited distinct methylation and transcriptional sensitivities to GR: the widely expressed direct GR target *fkbp5* and neuron-specific *aplp1*. In larvae, neural activity is required for GR-mediated transcription of *aplp1,* but not for that of *fkbp5*. GR regulates metabotropic glutamate receptor gene expression, the activities of which also modulated *aplp1* expression, implicating synaptic neurotransmission as an effector of GR function upstream of *aplp1*. Our results identify two distinct routes of GR-regulated transcription in the brain, including a pathway through which GR couples endocrine signalling to synaptic activity-regulated transcription by modulating metabotropic glutamate receptor expression.

Introduction

Interactions between an organism and its environment modify physiology and behaviour through co-ordinated changes to neural and endocrine signalling. Perception or anticipation of stressful sensory stimuli by the Central Nervous System (CNS) elicits a wide range of adaptive responses, including heightened cognition, altered affect, mobilisation of energy stores and the activation of locomotor responses (McEwen, 2012). Within the mammalian CNS, production of adaptive physiological responses to behavioural stressors is governed by interactions between the limbic system and the hypothalamo-pituitary-adrenal (HPA) axis (McEwen and Wingfield, 2010). Stress-induced activation of the HPA axis causes the adrenal gland to release glucocorticoid hormones into the circulation. In target cells, glucocorticoids bind to the Glucocorticoid Receptor (GR), a sequence-specific, DNA-binding transcription factor, inducing its translocation from the cytoplasm to the nucleus and thus facilitating its interactions with target DNA sequences (Kadmiel and Cidlowski, 2013).

Previous studies have identified targets of GR-mediated regulation and epigenetic control downstream of HPA axis activation (Gray et al., 2017; Sacta et al., 2016). In the zebrafish, a genetically and pharmacologically tractable model vertebrate, the GR regulates behaviour and the transcription of genes that function within the equivalent of the HPA axis, the hypothalamus-pituitary-interrenal (HPI) axis (Facchinello et al., 2017; Griffiths et al., 2012; Ziv et al., 2013). Many aspects of the molecular mechanisms through which the GR regulates genomic targets in the developing and adult brain have not yet been elucidated. In particular, it remains unclear how glucocorticoid signalling regulates genes that influence neural circuit

function. In order to obtain new insights into the impacts of GR function on epigenetic processes in the vertebrate brain, we carried out a comparative DNA methylome analysis of the brains of age-matched wild-type and mutant *gr*^{s357}adult male zebrafish. We hypothesised that GR target genes exhibit developmentally-regulated, glucocorticoid-sensitive patterns of DNA methylation in the brain. Moreover, since adaptive physiological and behavioural responses to environmental stressors require integration of endocrine and neural signalling activity within the central nervous system, we further hypothesised that signal integration is achieved at least in part through GR-mediated coupling of endocrine signalling to neural activity-dependent pathways of gene regulation. Our results support these hypotheses and yield novel insights into the molecular mechanisms through which endocrine signalling influences neural function.

Results

A loss-of-function mutation in the *nr3c1* gene encoding the zebrafish Glucocorticoid Receptor (GR), denoted *gr*^{s357}, was previously shown to cause abnormally high levels of HPI axis gene expression, elevated blood cortisol, and behavioural abnormalities suggestive of increased behavioural anxiety (Griffiths et al., 2012; Ziv et al., 2013). An initial analysis of locomotor behaviours and measurement of whole body cortisol of wild-type and *gr*^{s357} mutant adults and larvae supported and extended these findings (Figure 1), confirming a requirement for GR in regulation of both nervous and endocrine system functions in larval and adult stages. *gr*^{s357} mutant larvae and adults swam more slowly, larvae were more dispersed, and adults froze more frequently, were less exploratory and less dark aversive than age-matched wild-type animals (Figure 1 A-J). Moreover, *gr*^{s357} mutant larvae and adults had higher whole body cortisol levels than age-matched wild-type animals (Figure 1 K,L). These phenotypes suggested that the *gr*^{s357} mutant could be a tractable subject for elucidating the molecular mechanisms that integrate stress hormone signalling with neural activity-dependent processes. A wide range of studies have implicated epigenetic mechanisms as mediators of altered transcriptional responses to behavioural stressors (Gray et al., 2017; Zannas and Chrousos, 2017). To investigate the role of glucocorticoid signalling in the epigenetic regulation of neural stress responses in zebrafish, we analysed the DNA methylomes of wild-type and *gr*^{s357} mutant whole adult brain samples (Figure 2). Whole Genome Bisulfite Sequencing (WGBS) identified 249 genomic loci exhibiting differential methylation in the brains of *gr*^{s357} mutant and wild type males (Figure 2 Source Data 1). Gene Ontology analysis using the PANTHER Over-representation Test identified 14 GO

Terms within the Biological Process Category that were significantly associated with GR DMR-linked genes (Figure 2-figure supplement 1). Differentially Methylated Regions (DMRs) were ranked according to degree of differential methylation between genotypes (Figure 2 Source data 1), and a subset of high ranking DMRs linked to genes with biologically salient functional annotations were selected for confirmatory deep sequencing analysis in 10 additional wild-type and 10 *gr*^{s357} mutant adult male brains, using the BisPCR^2 technique (Bernstein et al., 2015). Of the 11 DMRs subjected to this analysis (Figure 2-figure supplement 2), only 3 of them exhibited significant differential methylation in whole brains of wild-type and *gr*^{s357} mutant adults (Figure 3A, Figure 4A, Figure 2-figure supplement 3, Figure 2-figure supplement 4, Figure 3-figure supplement 1A). A closely spaced cluster of three CpGs within the *fkbp5* intron 1 GR-DMR, and two CpGs within the *npepl1* intron 1 GR-DMR, were hypermethylated in *gr*^{s357} mutant compared to wild-type brains (Figure 3A, Figure 3-figure supplement 1A). In addition, two CpGs within a cluster located in the *aplp1* intron 1 GR-DMR were hypomethylated in *gr*^{s357} mutant compared to wild-type brains (Figure 4A). *Fkbp5* is a known direct target of the GR and encodes a protein which negatively regulates GR by tethering it in the cytoplasm in a complex with HSP90 (Zannas et al., 2016). Npepl1 is an M17 aminopeptidase with no known function (Matsui et al., 2006), and Aplp1 is a neuron-specific cell adhesion molecule closely related to Amyloid Precursor Protein (APP), which maintains dendritic spines and regulates basal synaptic neurotransmission (Schilling et al., 2017). The other 8 loci identified as putative DMRs by WGBS were not confirmed by BisPCR^2 deep sequencing analysis (Figure 2-figure supplement 4), and not studied further.

Genes harbouring or near to Glucocorticoid Receptor-regulated DNA methylation sites exhibit GR-regulated transcription in the adult brain

Having identified GR-sensitive DMRs that are significantly differentially methylated in adult wild-type and *gr*^{s357} mutant whole brain samples, the transcript abundance of the genes was investigated using qRT-PCR. Transcription of *fkbp5* was almost completely extinguished in *gr*^{s357} mutant brain tissue (Figure 3 B), whereas transcription of *aplp1* exhibited a robust ~12-fold increase in the *gr*^{s357} mutant (Figure 4B). The transcript abundance of *npepl1* was only slightly reduced by loss of GR function (Figure 3-figure supplement 1B). The considerable impacts of GR function on transcription of *fkbp5* and *aplp1* in the adult brain, together with the complementarity of their DNA methylation and transcriptional sensitivities to loss of GR function in this tissue, suggested that these two genes might be particularly informative subjects with which to investigate the molecular mechanisms downstream of glucocorticoid signalling *in vivo*.

The glucocorticoid-sensitivities of fkbp5 and aplp1 are regulated differentially by GR during zebrafish development

In order to investigate whether the GR-regulated DNA methylation and transcriptional sensitivities of *fkbp5* and *aplp1* that are apparent in the adult brain are established during development, methylation at the *fkbp5* and *aplp1* DMRs were measured in wild-type and *gr*^{s357} mutant embryos at the blastula stage, before the onset of zygotic gene transcription, and in free-swimming wild-type and *gr*^{s357} mutant

5 d.p.f. larvae. The pharmacological tractability of zebrafish larvae also enabled us to investigate the impacts of exogenous glucocorticoid treatment on DNA methylation and transcription of *fkbp5* and *aplp1*, using the synthetic glucocorticoid betamethasone, which is a selective agonist of the GR (Grossmann et al., 2004). None of the CpGs within the *fkbp5* GR-DMR showed any difference in their levels of methylation in wild-type and *gr*^{s357} mutant blastulae (Figure 3C). However, in dissected 5 d.p.f larval head tissue, the CpGs within the *fkbp5* GR-DMR exhibited complementary changes in methylation level in response to exogenous glucocorticoid and loss of GR function (Figure 3D). Thus, betamethasone exposure reduced the level of methylation of the *fkbp5* GR-DMR in wild-type larvae, whereas methylation of the fkbp5 GR-DMR was increased in gr^{s357} mutant larvae, and this increase persisted when gr^{s357} mutant larvae were exposed to betamethasone. Moreover, the glucocorticoid-sensitive and GR-dependent methylation changes observed within the fkbp5 GR-DMR were accompanied by complementary increases in *fkbp5* transcript abundance in wild-type larvae exposed to glucocorticoid, or strongly reduced transcription in both untreated and glucocorticoid-treated *gr*^{s357} mutant larvae, at both 3 d.p.f. and 5 d.p.f. (Figure 3E). Whole-mount *in situ* hybridisation analysis of *fkbp5* transcription in 5 d.p.f. larvae confirmed that transcripts were expressed at low levels in untreated wild-type larvae and strongly induced by betamethasone treatment, but completely undetectable in *gr*^{s357} mutant larvae, whether they were exposed to betamethasone or not (Figure 3F). Taken together, these results demonstrate that in the larval and the adult zebrafish brain, glucocorticoid signalling mediated via the DNA binding function of GR promotes transcription of *fkbp5* and reduces methylation of a cluster of CpGs within intron 1 of this gene.

Within the *aplp1* intron 1 GR-DMR, all six of its CpGs were nearly fully methylated in wild-type and *gr*^{s357} mutant blastulae (Figure 4C). This high level of CpG methylation persisted in in 5 d.p.f. wild-type and *gr*^{s357} mutant larvae, whether they were exposed to exogenous glucocorticoid or not (Figure 4D). However, *aplp1* transcription was strongly induced in wild-type larvae by exogenous glucocorticoid, but not in *gr*^{s357} mutant larvae, at both 3 d.p.f. and 5 d.p.f. (Figure 4E). *In situ* hybridisation analysis revealed that GR-independent, basal expression of *aplp1* is restricted to the developing larval brain (Figure 4F). Exposure of wild-type larvae to exogenous glucocorticoid increased *aplp1* expression throughout the brain, but this increase was not observed in *gr*^{s357} mutant larvae (Figure 4F). Thus, at larval stages, glucocorticoid signalling through the GR robustly induced transcription of *aplp1* without modifying methylation of its GR-sensitive DMR.

Glucocorticoid-inducible transcription of aplp1, unlike fkbp5, is insensitive to functional inhibition of the GR co-chaperone protein Fkbp5

Our experimental findings suggested that there are important differences in the molecular mechanisms that determine CpG methylation of the *fkbp5* and *aplp1* GR-DMRs and the transcriptional responses of these two genes to glucocorticoid signalling. Through a direct interaction with GR, the Fkbp5 protein has been shown to set the concentration of glucocorticoid required to promote nuclear import of GR to regulate target gene transcription (Galat, 2013; Wochnik et al., 2005; Zannas and Binder, 2014). To investigate whether this buffering function of the Fkbp5 protein limits the transcriptional responses of *fkbp5* and *aplp1* genes to exogenous

glucocorticoid, the small molecules FK506 and SAFit2 (Gaali et al., 2015) were used to inhibit Fkbp5 function in wild-type and *gr*^{s357} mutant larvae, and the responsiveness of *fkbp5* and *aplp1* to a subsequent betamethasone exposure was then measured by qRT-PCR. FK506 inhibits multiple FKBPs that include Fkbp5 and Fkbp4, whereas SAFit2 is a highly specific inhibitor of Fkbp5 (Gaali et al., 2015; Zannas and Binder, 2014). 4 d.p.f. larvae were exposed to 1μM FK506 (Figure 5A,B) or to 100nM SAFit2 (Figure 5C,D) alone for 1 hour, after which betamethasone was then added to the medium at final concentrations of 5, 10, 20, 50, or 100 μM for a further 2 hours. Both FK506 and SAFit2 robustly enhanced the glucocorticoid concentration-dependent induction of *fkbp5* transcription in wild-type larvae, whereas *fkbp5* transcription in *gr*^{s357} mutant larvae was completely unresponsive to FK506, SAFit2 and betamethasone (Figure 5A,C). Thus, in the larval brain, the FK506/SAFit2 protein target Fkbp5 buffers the responsiveness of the *fkbp5* gene to the available concentration of glucocorticoid, and when Fkbp5 function is inhibited, the transcriptional response of *fkbp5* to glucocorticoid is enhanced. By contrast, exposure of 4 d.p.f. larvae to FK506 and SAFit2 had no effect on the sensitivity or magnitude of the glucocorticoid concentration-dependent induction of *aplp1*, which was, nevertheless strictly dependent on GR function (Figure 5B,D). Moreover, the responsiveness of *aplp1* to glucocorticoid treatment exhibited a sharper, more discontinuous, threshold-like response, in comparison to the qualitatively distinct, more graded transcriptional response of *fkbp5* to glucocorticoid. These results suggest that whilst GR-mediated, glucocorticoid-induced transcription of *fkbp5* is buffered by available Fkbp5 protein function, *aplp1* transcription is not constrained by Fkbp5. We conclude that *aplp1* is regulated by a GR-dependent mechanism distinct from that which regulates the responsiveness of *fkbp5* to glucocorticoid signalling.

Synaptic activity acts downstream of glucocorticoid signalling in zebrafish larvae to regulate transcription of aplp1 but not methylation of the aplp1 GR-DMR

Our studies show that *aplp1* is specifically expressed in the zebrafish brain and that glucocorticoid-induced, GR-dependent transcription of *aplp1* is not buffered by Fkbp5 protein function (Figure 5B,D), unlike that of *fkbp5*. Together with the known functions of Aplp1 in maintaining dendritic spines and promoting synaptic activity (Schilling et al., 2017), these findings suggested that transcriptional regulation of *aplp1* is mechanistically distinct from that of *fkbp5* and might represent a site for functional integration of glucocorticoid and synaptic signalling within the larval brain. To investigate whether neural activity modulates glucocorticoid-induced transcription of *aplp1* and *fkbp5,* we used CRISPR/Cas9 to create a loss-of-function mutation in *stxbp1a,* which is specifically expressed in neurons (Figure 6A), and required for synaptic neurotransmission (Grone et al., 2016). A loss-of-function allele was generated, *stxbp1a*^{sh438}, in which a 15 bp deletion combined with a 5 bp insertion destroyed the exon 8 - intron 8 splice junction (Figure 6B). Consistent with previously published observations on other *stxbp1a* alleles *(*Grone et al., 2016), homozygous *stxbp1a*^{sh438} mutants appear morphologically normal but they are immotile (Figure 6C). *stxbp1a*^{sh438} mutants also lack neural activity when measured by patch clamping of individual neurones (Figure 6D). When the neural activity reporter transgene *NBT:GCaMP3* was introduced into the *stxbp1a*^{sh438} mutant line, imaging of GCaMP3 fluorescence in 3 d.p.f. larvae (Bergmann et al., 2018) further confirmed a lack of neural activity within the *stxbp1a*^{sh438} mutant larval brain (Figure 6E, Figure 6 – video 1, Figure 6 – video 2). Moreover, exposure of homozygous *stxbp1a*^{sh438}

mutant larvae to the neural activity-inducing compound Pentylenetetrazole (PTZ) also failed to elicit increased locomotor movements, more frequent action potentials, or widespread transcription of the synaptic activity-regulated gene *cfos* in the brain, as was observed in wild-type siblings (Figure 6C,D,F). To determine whether the two distinct modes of glucocorticoid-inducible transcription of *aplp1* and *fkbp5* were affected by loss of *stxbp1a* function, we compared *aplp1* and *fkbp5* transcription in 4 d.p.f. wild-type and *stxbp1a*^{sh438} mutant larvae exposed to exogenous glucocorticoid, in the presence or absence of the specific Fkbp5 inhibitor SAFit2 (Figure 7). Wild-type larvae exhibited a robust, glucocorticoid concentration-dependent induction of *aplp1* transcription, which was insensitive to SAFit2, whereas the inducibility of *aplp1* was extinguished in *stxbp1a*^{sh438} mutant larvae (Figure 7A). In striking contrast, glucocorticoid concentration-dependent induction of *fkbp5* transcription was enhanced by SAFit2 and remained unchanged by homozygosity for the *stxbp1a*^{sh438} mutation (Figure 7B). Thus, in the larval brain, *stxbp1a*-dependent synaptic signalling renders *aplp1* competent for transcriptional activation by glucocorticoid in an Fkbp5-independent manner, but *stxbp1a* is not required for glucocorticoid-induced, Fkbp5-buffered transcription of the *fkbp5* gene. In order to determine whether the methylation levels of CpGs within the *aplp1* and *fkbp5* GR-DMRs were sensitive to glucocorticoid signalling in the absence of *stxbp1a* function, their percentage methylation in larval head tissue was compared in 4 d.p.f. wild-type and homozygous *stxbp1a*^{sh438} mutant larvae, after exposure to exogenous glucocorticoid. The high level of methylation of all 6 CpGs within the *aplp1* GR-DMR was unaltered by loss of *stxbp1a* function at any of these CpGs, and remained unchanged after exposure of either wild-type or *stxbp1a*^{sh438} mutant larvae to exogenous glucocorticoid (Figure 7C). However, methylation of all 4 CpGs within the *fkbp5* GR-DMR was reduced by

exposure of either wild-type or *stxbp1a*^{sh438} mutant larvae to exogenous glucocorticoid (Figure 7D). Taken together, our results indicate that the induction of *aplp1* transcription by glucocorticoid signalling requires *stxbp1a*-dependent synaptic activity but is unbuffered by Fkbp5 protein function, and that methylation of the *aplp1* DMR is unaffected by loss of *stxbp1a* function. By contrast, the induction of *fkbp5* transcription by glucocorticoid does not require *stxbp1a* function, and this inducibility is buffered by existing levels of Fkbp5 protein. Moreover, exogenous glucocorticoid caused hypomethylation of the *fkbp5* DMR independently of *stxbp1a* function.

To investigate whether increased levels of excitatory synaptic activity could directly induce transcription of *aplp1* and *fkbp5* downstream of glucocorticoid signalling, wild-type and *gr*^{s357} mutant larvae were exposed to the neural activity-inducing convulsant agent PTZ or control medium for 90 minutes, and the expression levels of *aplp1* and *fkbp5* were then determined by qRT-PCR. The results show that *aplp1* transcription is induced by PTZ in both wild-type and *gr*^{s357} mutant larvae (Figure 7E). By contrast, *fkbp5* mRNA was not induced by PTZ treatment, but the low basal level of transcription was nevertheless strictly dependent on wild-type GR function (Figure 7F). These results indicate that synaptic activity acts downstream of GR function in zebrafish larvae to promote *aplp1* transcription in response to glucocorticoid signalling without modulating methylation at the *aplp1* GR-DMR. In contrast, glucocorticoid-induced *fkbp5* transcription is accompanied by reduced methylation of all four CpGs within the *fkbp5* GR-DMR, and is independent of synaptic activity in the larval CNS.

The Glucocorticoid Receptor regulates metabotropic glutamate receptor expression upstream of aplp1

Glucocorticoids are well-documented regulators of glutamatergic signalling (Popoli et al., 2011; Treccani et al., 2014), and recently published evidence suggests roles for stress-induced glucocorticoid signalling in the regulation of metabotropic glutamate receptor expression (Nasca et al., 2015a; Nasca et al., 2015b). We compared expression of all known metabotropic glutamate receptor genes in wild-type and *gr*^{s357} mutant zebrafish, and found that expression of the Group II genes *grm2a, grm2b, grm3* and the Group I gene *grm5a* exhibited clear-cut sensitivities to loss of GR function (Figure 8). In the adult brain, loss of GR function reduced expression of *grm2a*, *grm2b,* and *grm3,* whereas expression of *grm5a* was increased (Figure 8A). In *gr*^{s357} mutant larvae, expression of *grm2a, grm2b* and *grm3* was similarly reduced, and expression of *grm5a* was increased (Figure 8B). Moreover, exposure of wild-type larvae to exogenous glucocorticoid increased *grm2a*, *grm2b,* and *grm3* expression but decreased expression of *grm5a*, in a GR-dependent manner (Figure 8B). Next, we investigated whether transcriptional responses of *grm2a, grm2b, grm3* and *grm5a* to glucocorticoid signalling were affected by loss of *stxbp1a* function. We observed that exogenous glucocorticoid elicited increased expression of *grm2a*, *grm2b,* and *grm3* equally in *stxbp1a*^{sh438} mutant larvae and in their wild-type siblings Figure 8C), but the glucocorticoid-suppressible expression of *grm5a* observed in wild-type larvae was abrogated in *stxbp1a*^{sh438} mutants. These results suggest that GR promotes glucocorticoid-induced transcription of *grm2a, grm2b* and *grm3* in presynaptic neurones independently of *stxbp1a* function, and that glucocorticoid-suppressible *grm5a* transcription in post-synaptic neurones involves synaptic activity

requiring *stxbp1a* function. To determine whether Grm2a, Grm2b, Grm3 and Grm5a activities might regulate *aplp1* expression downstream of GR, wild-type and *gr*^{s357} mutant larvae were exposed to the Grm2a/Grm2b/Grm3 agonist LY354740 and/or the Grm5 antagonist SIB-1893. Both LY354740 and SIB-1893 treatments caused similar increases in *aplp1* mRNA levels that were additive, in wild-type and *gr*^{s357} mutant larvae (Figure 9A). Treatment of wild-type larvae with exogenous glucocorticoid alone, or after exposure to LY354740 and/or SIB-1893, robustly induced *aplp1* to a higher level than could be achieved with LY354740 and/or SIB-1893 alone, but this increase was abolished in *gr*^{s357} mutant larvae (Figure 9A). However, when phenotypically wild-type sibling and homozygous *stxbp1a*^{sh438} mutant larvae were treated with Grm2a/Grm2b/Grm3 agonist LY354740, only wild-type sibling larvae exhibited significantly increased *aplp1* expression (Figure 9B), indicating that synaptic activity is required for LY354740 to enhance *aplp1* transcript levels post-synaptically. By contrast, the Grm5a antagonist SIB-1893 enhanced *aplp1* transcript abundance in both wild-type sibling and *stxbp1a*^{sh438} mutant larvae, confirming that *aplp1* expression was increased by Grm5a inhibition in post-synaptic cells (Figure 9B). As was observed for *gr*^{s357} mutant larvae, *aplp1* transcription remained unresponsive to exogenous glucocorticoid in *stxbp1a*^{sh438} mutant larvae, whilst wild-type larvae treated with exogenous glucocorticoid alone, or after exposure to LY354740 and/or SIB-1893, robustly induced *aplp1* to a much higher level than was observed with LY354740 and/or SIB-1893 alone. Taken together, these results indicate that glucocorticoid signalling via the GR increases Group II metabotropic glutamate receptor expression, decreases expression of the Group I receptor Grm5a, and induces *aplp1* transcription in postsynaptic neurones of the larval brain. Furthermore, a pharmacological activator of Group II metabotropic glutamate

receptors acts downstream of GR but upstream of Stxbp1a to promote *aplp1* expression post-synaptically, whereas a pharmacological inhibitor of the Group I receptor Grm5a functions downstream of both GR and Stxbp1a, post-synaptically, to enhance *aplp1* transcription.

Discussion

GR regulates neural gene transcription and DNA methylation dynamics in zebrafish larvae and adults

Adaptive responses to environmental stressors require integration and modulation of endocrine and neural signals within the central nervous system. We hypothesised that glucocorticoid signalling mediated by GR regulates specific epigenetic and transcriptional networks in the brain that regulate behavioural responses to stress. Our studies of the epigenetic and transcriptional impacts of glucocorticoid signalling mediated by the Glucocorticoid Receptor support this hypothesis. Our DNA methylation analysis of the brains of wild-type and gr^{s357} mutant adults identified GR-sensitive DMRs within the first introns of *fkbp5* and *aplp1*, which are accompanied by GR-dependent changes in the transcription of these genes in the brain. In gr^{s357} mutant adult brains, methylation levels were increased at three of four CpGs within the *fkbp5* DMR and transcription of *fkbp5* was extinguished. Conversely, two of six CpGs within the *aplp1* DMR exhibited decreased methylation in gr^{s357} mutant adult brains, and *aplp1* transcription was increased by more than 12-fold. These methylation changes likely reflect transcriptional regulatory functions of DNA

sequences within the identified GR-DMRs that could contribute to the GR-dependent transcriptional changes we have identified for *fkbp5* and *aplp1*. The fractional changes in the level of methylation at the *fkbp5* and *aplp1* DMRs indicate that for both genes, the observed methylation changes occur in relatively small proportions of the adult brain samples that were analysed. These findings contrast with the large changes in transcript abundance observed in adult brain tissue samples and in wild-type larvae exposed to exogenous glucocorticoid (Figures 3 and 4), raising the possibility that, for both *fkbp5* and *aplp1*, there are other, as yet unidentified, DMRs within or near to these genes that could also exhibit glucocorticoid sensitivity in distinct neuronal populations and contribute to the glucocorticoid-inducibility of these genes.

We were surprised to discover that a majority of the 11 DMRs identified by WGBS exhibited no significant difference in the level of DNA methylation in wild-type and gr^{s357} mutant adult brains subjected to deep sequence analysis using the BisPCR^2 technique (Figure 2-figure supplement 4). These differences are likely to be due, at least in part, to the different sensitivities of the two techniques. Whilst the WGBS analysis was genome-wide, it provided only a small number of reads per sample for any given CpG within the genome. By contrast, the BisPCR^2 analysis was targeted at a small number of specific CpGs within specific DMRs in great depth, typically yielding many thousands of reads per CpG per tissue sample. Given the considerable tissue complexity and neuronal heterogeneity within the adult brain, limited-depth WGBS would thus be expected to reveal the methylation state for any given CpG in only a small number of cells from any given tissue sample, whereas the greater sequencing depth of the BisPCR^2 analysis provides a much more

representative indication of the overall percentage methylation of selected CpGs, within a larger proportion of the cell population under analysis.

GR-dependent, glucocorticoid-induced transcription of fkbp5 is accompanied by reduced methylation of the fkbp5 GR-DMR in zebrafish larvae and adults

The absence of *fkbp5* mRNA in the zebrafish adult *gr*^{s357} mutant brain confirms that GR activates transcription of *fkbp5* in this tissue. The ability of exogenous glucocorticoid to suppress methylation of the *fkbp5* GR-DMR in larvae, and co-ordinately induce *fkbp5* transcription in a GR-dependent manner, further suggests that in a subset of neural cells, GR actively drives transcription-linked demethylation at the GR-DMR, raising the possibility that GR function leads to the recruitment of one or more TET demethylases that promote *fkbp5* transcription in these cells. Sequence analysis of the *fkbp5* promoter reveals the presence of three Glucocorticoid Response Elements (GREs) within a 200bp region located 100-300bp from the transcription start site (Figure 10). Analysis of the *fkbp5* GR-DMR sequence indicates similarities with binding sites for the transcription factors RHOXF1, CREB1, JUND, NR2F1, RXRA, and PAX4, recruitment of which may be regulated by the GR-dependent demethylation of the GR-DMR we have identified. Associations are known between variation in *cis*-regulatory DNA sequences within the human *FKBP5* gene and human psychiatric disorders (Criado-Marrero et al., 2018). The DNA sequence polymorphism *rs1360780*, located within intron 2 of the human *FKBP5* gene, modulates *FKBP5* demethylation, transcription, and susceptibility to stress-related psychiatric disorders (Klengel et al., 2013). Further analysis of the GR-DMR

we have identified within intron 1 of the zebrafish *fkbp5* gene may also help to understand the relationships between GR function, DNA demethylation, *fkbp5* transcription, and the pathobiology of such affective disorders.

Synaptic activity mediates GR-dependent induction of aplp1 transcription in the zebrafish larval brain via a metabotropic glutamate receptor-regulated pathway

In the *gr*^{s357} mutant adult brain, loss of GR function caused a robust increase in *aplp1* transcription, together with the decreased methylation at adjacent CpGs within the *aplp1* GR-DMR, demonstrating that GR is involved in attenuating transcription of *aplp1* and promoting DNA methylation of the *aplp1* GR-DMR in the adult wild-type brain. By contrast, in wild-type larvae, *aplp1* transcription was glucocorticoid-inducible, but its GR-DMR was hypermethylated and unresponsive to glucocorticoid treatment. The *aplp1* GR-DMR of *gr*^{s357} mutant larvae exhibited the same degree of methylation as in wild-type larvae and was similarly unresponsive to glucocorticoid treatment. Moreover, loss of GR-function did not cause the substantial transcriptional de-repression of *aplp1* in *gr*^{s357} mutant larvae, that was observed in the *gr*^{s357} mutant adult brain. These results indicate that whilst GR mediates the glucocorticoid inducibility of *aplp1* in larvae, in the adult brain it functions as a direct or indirect transcriptional repressor of *aplp1*. Such distinct properties at different stages of development might be the result of neural adaptations resulting from exposure to external stimuli encountered across the life course, and/or the development of neuronal structures in the adult brain in which the function of GR is different to that

performed in the simpler larval brain. In mammals, Aplp1 is a transmembrane-spanning homotypic cell adhesion molecule closely related to the Amyloid Precursor Protein (APP), that is localized to both pre- and post-synaptic membranes, where it stabilizes dendritic spines, promotes basal neurotransmission and is sensitive to proteolysis by gamma-secretase (Ludewig and Korte, 2016; Schauenburg et al., 2018; Schilling et al., 2017). Neural activity-induced changes in *aplp1* expression in the zebrafish brain might thus modulate synapse structure and function, facilitating neural circuit remodelling in response to changes in sensory input. JASPAR analysis of the DNA sequence corresponding to the *aplp1* GR-DMR indicated that the differentially methylated CpGs lie within an E-box-like potential binding site for bHLH transcriptional regulators, including the Aryl hydrocarbon-regulated Ahr/ARNT, Notch-regulated transcription factors Hes1/Hey1/Hey2, the hypoxia-regulated transcription factor HIF1, the cell cycle regulators Myc and Nmyc, and Tcfl5 (Figure 10). Whilst there are no apparent GREs in the *aplp1* promoter, a single putative GRE is located at nucleotides 15:37257059-15:37257074, 7004 nucleotides away from the *aplp1* GR-DMR that could potentially mediate a direct interaction between GR and the *aplp1* gene.

Our comparison of the impacts of pharmacological inhibitors of Fkbp5 function on the glucocorticoid inducibility of *fkbp5* and *aplp1* in wild-type and gr^{s357} mutant larvae indicated that transcription of *fkbp5* was enhanced by Fkbp5 inhibition, whereas that of *aplp1* was not. This difference, together with the neural-specific expression pattern of *aplp1*, suggested that the mechanisms regulating glucocorticoid-induced transcription of *fkbp5* and *aplp1* are distinct. Remarkably, in $stxbp1a^{sh438}$ homozygous mutant larvae, transcription of *fkbp5* remained fully glucocorticoid-inducible, whereas, *aplp1* transcription did not respond to glucocorticoid treatment,

demonstrating that the synaptic activity enabled by Stxbp1a function is required downstream of GR activity to permit glucocorticoid-induced *aplp1* transcription. Furthermore, treatment of larvae with the neural activity-inducing $GABA_A$ receptor antagonist PTZ strongly induced *aplp1* transcription in both wild-type and gr^{s357} mutant larvae, whilst PTZ was unable to elicit *fkbp5* transcription in either wild-type or gr^{s357}mutant larvae. These complementary results confirm that the molecular mechanisms mediating glucocorticoid-induced transcription of *fkbp5* and *aplp1* in zebrafish larvae are qualitatively distinct, and demonstrate that neural activity acts downstream of glucocorticoid signalling to induce *aplp1* transcription.

Many studies have shown that glucocorticoid signalling can regulate glutamate release within the mammalian CNS (Popoli et al., 2011). The mGlur2 metabotropic glutamate receptor has recently been shown to function downstream of glucocorticoid signalling in the mouse hippocampus (Nasca et al., 2015a). We found that GR promotes transcription of the zebrafish Group II *grm* genes *grm2a, grm2b,* and *grm3,* and represses the Group I gene *grm5a,* in both adult brain and larval head tissue samples. Moreover, in the larval brain, *grm2a, grm2b* and *grm3* were induced by exogenous glucocorticoid, whereas *grm5a expression* was inhibited by glucocorticoid (Figure 8). The loss of *grm5a* expression in $stxbp1a^{sh438}$ mutant larvae further indicates that expression of *grm5a* lies downstream of the post-synapse.

We found that a pharmacological agonist of Grm2a/Grm2b/Grm3, and a pharmacological antagonist of Grm5a both increased transcription of *aplp1* in wild-type and gr^{s357}mutant larvae, suggesting that these metabotropic glutamate receptors independently modulate synaptic activity downstream of GR function and upstream of *aplp1*. Furthermore, whilst the Grm5a antagonist SIB-1893 increased

509 *aplp1* expression in *stxbp1a*^{sh438} mutant larvae, the Group II Receptor agonist
510 LY354740 did not. On the basis of these results, we propose a model in which
511 glucocorticoid-bound GR promotes *grm2a, grm2b* and *grm3* expression
512 presynaptically, whilst it attenuates *grm5a* expression and stimulates *aplp1*
513 transcription post-synaptically (Figure 11). Our results further indicate that
514 presynaptic Grm2a/Grm2b/Grm3 activity promotes *aplp1* transcription post-
515 synaptically, and that transcription of *aplp1* is limited by Grm5a activity in
516 postsynaptic neurons. It is possible that exposure to exogenous glucocorticoids
517 triggers release of excitatory and/or inhibitory neurotransmitters from presynaptic
518 terminals in the larval CNS, and it seems likely that the *grm* genes we have identified
519 play important roles in regulating synaptic plasticity in response to such
520 glucocorticoid signalling, by modulating expression of *aplp1* and potentially other
521 synapse components. Future studies will explore these possibilities and further
522 elucidate the biological function of the *GR-Grm-Stxbp1a-Aplp1* pathway that we have
523 identified.
524
525
526

Materials and Methods

Zebrafish Husbandry

Adult zebrafish were maintained with a 14 h light/10 h dark cycle at 28ºC according to standard protocols and were mated using spawning tanks. The *nr3c1* mutant allele *gr*^{s357} (Ziv et al., 2013) was obtained from Herwig Baier (MPI for Neurobiology, Martinsried, Germany) and zebrafish were genotyped at the *nr3c1* locus by sequencing genomic DNA-derived PCR products encompassing the *s357* mutation. Homozygous mutant and wild-type sibling adult populations were created by in-crossing adult *gr*^{s357} heterozygotes, and the resulting larvae were raised to adulthood. Young adults were genotyped by fin-clipping to establish groups of homozygous wild-type and homozygous *gr*^{s357} mutant fish, which were maintained in separate tanks and then used for behavioural and molecular analysis. Larvae for experimental analysis were obtained from in-crosses of wild type and homozygous mutant adult siblings. Larvae were maintained in petri dishes containing E3 medium at 28.5°C and staged according to Kimmel's guide (Kimmel et al., 1995). All procedures involving experimental animals were performed in compliance with local and national animal welfare laws, guidelines and policies. Adult zebrafish were analysed aged 11-15 months and larvae aged up to 5 d.p.f. Brains used for WGBS and targeted bisulfite sequencing, and adult body samples for steroid extraction were from males, whilst other experiments used equal numbers of males and females. Heterozygous *stxbp1a*^{sh438} mutant adults were in-crossed to produce *stxbp1a*^{sh438} homozygous mutant larvae and phenotypically wild-type sibling larvae for experimental analysis.

552

553 *Behavioural analysis*

554 Zebralab and Shoaling softwares (Viewpoint, France) were used to track the
555 movement of individual zebrafish when isolated and in shoals respectively, to
556 provide quantitative measures of swimming behaviour, as previously described
557 (Eachus et al., 2017). Locomotor activity of 3 d.p.f. *stxbp1a*^{sh438} homozygous mutant
558 and sibling larvae, maintained in the presence or absence of 5mM
559 Pentylenetetrazole, was measured over a 1 hour period in the Zebrabox (Viewpoint,
560 France), as previously described (Baxendale et al., 2012).
561 *Open field test*: individual fish were acclimated to the empty tank, horizontal
562 swimming behaviour was then recorded for 10 minutes, as previously described
563 (Eachus et al., 2017).
564 *Tank diving test*: vertical swimming behaviour of individual fish was recorded and
565 binned at 1 minute intervals in a 10 minute test, as previously described (Eachus et
566 al., 2017).
567 *Scototaxis test*: horizontal swimming behaviour of individual fish, performed in the
568 light half of the tank, was recorded in a 10 minute test and binned every 1 minute, as
569 previously described (Eachus et al., 2017).
570 *Shoaling analysis of larvae*: shoals of 21 larvae aged 5.d.p.f were transferred to a
571 circular petri dish and horizontal swimming behaviour was then recorded for 10
572 minutes as previously described (Eachus et al., 2017).

573

574 *Extraction and quantification of cortisol*

575 Individual adult zebrafish were culled via a rapid overdose of Tricaine followed by
576 decapitation and the body was snap frozen for cortisol extraction. Larval cortisol

samples were collected from pools of 21 larvae aged 5 d.p.f., which were snap frozen in an Eppendorf tube. Cortisol was extracted using previously described protocols for adult and larval zebrafish respectively (Cachat et al., 2010; Yeh et al., 2013). Whole body cortisol was then quantified using the ELISA protocol previously described (Cachat et al., 2010; Yeh et al., 2013).

Quantitative RT-PCR

Pools of dissected larval heads or whole larvae were snap frozen at 3, 4 or 5 d.p.f.. RNA extraction, cDNA synthesis and qRT-PCR were carried out as previously described (Eachus et al., 2017).

In situ hybridisation

Whole-mount *in situ* hybridisation on larvae was performed according to standard protocols (Boyd et al., 2015). Details of plasmids used to generate Digoxigenin-labelled RNA *in situ* hybridization probes for *fkbp5, aplp1, stxbp1a* and *cfos* are available on request.

Whole Genome Bisulfite Sequencing

Whole brains (two wild type and two gr^{s357} mutant) were dissected from adult zebrafish and genomic DNA was extracted using the Qiagen DNAeasy kit. DNA sequencing libraries were prepared and sequenced using 125 bp paired end reads on an Illumina Hiseq by GATC Biotech. Sequence data quality was inspected using FastQC and reads were trimmed to phred-quality Q15. Reads were aligned to the reference genome (*Danio rerio*, GRCz10 release 85) using Bismark with the default parameters (Krueger and Andrews, 2011). PCR duplicates were removed and

methylation calls were made using Bismark v0.15.0. Regions that were differentially methylated in mutants were detected using the bsseq R package v1.8.2 with default parameters: the data were smoothed, low coverage (<2x coverage in all samples) CpGs were removed, t-statistics were computed and thresholded at 4.6 to identify differentially methylated CpGs (https://support.bioconductor.org/p/78227/). The WGBS DNA sequence data and associated metadata are available at the NCBI Gene Expression Omnibus under Accession Number GSE120632.

Gene Ontology (GO) analysis of the genes lying adjacent to or harbouring DMRs were carried out using PANTHER (Mi et al., 2013).

Methylation heatmaps were constructed using DeepTools (v3.1.3). Genes were scaled to 10 000 bp and methylation was averaged in 250 bp bins. Methylation was plotted for 1448 genes exhibiting >95% CpG coverage within the interval spanning 5kb upstream of the Transcription Start Site (TSS), the gene body and 5kb downstream of the Transcription Termination Site (TTS), for wild-type and *gr*^{s357} mutant samples.

Targeted BS-PCR using the BisPCR^2 method

Whole brains (from ten wild type and ten mutant adult fish ~ 1 year in age) were dissected from adult zebrafish and genomic DNA was extracted using the Qiagen DNAeasy kit. Library preparation was based on previously published protocols (Bernstein et al., 2015). ~200 ng of each DNA sample was bisulfite treated using the Qiagen Epitect kit, according to the kit instructions, and quantified using an Agilent Tapestation with High-sensitivity tape.

100pg bisulfite-converted DNA was amplified for 40 cycles in PCR round 1, using KAPA Hifi Uracil+ Readymix with 300nM primer. The optimum annealing

temperature and MgCl2 concentration for each primer pair were determined by analysing PCR products on a 2% agarose gel. The PCR round 1 primers included a 25-30 bp amplicon-specific sequence, designed using MethPrimer (Bernstein et al., 2015) plus an 18 bp overhang to allow the annealing of PCR round 2 primers. All PCR round 1 amplicons were pooled for each individual sample at 10 ng/amplicon based on quantification via the Agilent Tapestation. Excess primers and dNTPs were removed using the Qiagen PCR clean-up kit. Individual samples were then barcoded via a second round of PCR. PCR round 2 reactions were 20ul, using the KAPA Hifi Uracil+ mastermix, with 300 nM primer and 1 ng of pooled PCR round 1 product for each sample. The PCR round 2 forward primer was identical to the 5' overhang on the PCR round 1 amplicons, whilst the reverse primer included a region to anneal to the 3' overhang on the PCR round 1 amplicons, plus a 6 bp sample-specific barcode. The final barcoded amplicons ranged from 199-270 bp. Excess primers and dNTPs were removed using the Qiagen PCR clean-up kit. Sample quantity and size was determined using the Agilent Tapestation. Products outside of the expected range were removed using AMPure XP beads. Samples were then pooled in an equimolar manner, and a 500 ng pool was shipped to GATC Biotech for sequencing. Illumina adapters were ligated by GATC Biotech and the samples were sequenced on the Illumina Hiseq for 150 bp paired end reads.

Sequence quality was determined using FastQC (http://www.bioinformatics.babraham.ac.uk/projects/fastqc). Sequence data was demultiplexed using QIIME 1 (Caporaso et al., 2010; Li and Dahiya, 2002) and primers were trimmed using cutadapt (https://journal.embnet.org/index.php/embnetjournal/article/view/200). Data was

aligned to the reference genome (*Danio rerio*, GRCz10 release 85) and methylation levels were called using BSseeker2 (Guo et al., 2013).

Creation of mutations in stxbp1a using CRISPR/Cas9 gene editing

The CRISPR/Cas9 gene editing approach was used to induce targeted mutations at the *stxbp1a* locus (Hwang et al., 2013; Sander et al., 2010). To induce mutations in *stxbp1a*, an *stxbp1a*-specific ultramer was designed, using the ZiFit Targeter (http://zifit.partners.org/ZiFiT/), having the following DNA sequence:

5′AAAGCACCGACTCGGTGCCACTTTTTCAAGTTGATAACGGACTAGCCTTATTTTAACTTG

CTATTTCTAGCTCTAAAAC***CCATTGTAGG*ATCATCTGCC**CTATAGTGAGTCGTATTACGC3′

The *stxbp1a*-specific 20-mer target sequence (highlighted in bold) includes 10 of 11 nucleotides corresponding to a BslI recognition site (italics) and lies adjacent to the T7 promoter sequence (underlined). The *stxbp1a*-specific Ultramer was annealed to a short oligonucleotide complementary to its T7 promoter sequence, and an *stxbp1a*-specific Cas9 guide RNA (gRNA) was then synthesized in vitro using the MEGAshortscript T7 kit (life Technologies). Cas9 mRNA was similarly synthesized by *in vitro* transcription and combined with gRNA in water. 1 cell embryos were injected with 2-4nl of a CRISPR/Cas9 RNA mixture containing 2.4μg/μl gRNA and 0.5μg/μl Cas9 mRNA in water. A proportion of injected embryos were collected after one day of development and analysed for mutagenesis of the targeted *stxbp1a* exon 8 using PCR and a BslI restriction digest of the 214bp PCR amplicon, which identified BslI-insensitive mutant alleles. PCR primers for amplification of exon 8 were:

5′-ACAGATGTCCAGTAGTCTCGG-3′ (STXBP1A3F), and

675 **5′-TTTCTCTCTCCCTGCAGTGC-3′** (STXBP1A3R). Other CRISPR/Cas9-injected
676 embryos were raised to adulthood and these F_0 fish were then outcrossed to wild-
677 type AB adults to produce F_1 progeny. Genomic DNA was isolated from F_1 individual
678 embryos and subjected to PCR to identify F_0 animals transmitting BslI-insensitive
679 *stxbp1a* exon 8 alleles to F_1 progeny. Mutations were identified by DNA sequencing
680 of BslI-insensitive amplicons. F_0 adult transmitters of BslI-insensitive *stxbp1a* exon 8
681 alleles were further outcrossed to AB stocks and F_1 germline heterozygous adults
682 were raised and genotyped by fin clipping to establish mutant lines. These
683 experiments led to the identification of the stxbp1a^{sh438} allele, which was named
684 using the “sh” designation for University of Sheffield, in accordance with the
685 published ZFIN guidelines.
686
687 *Pharmacological manipulation of embryos and larvae*
688 Betamethasone (BM) and FK506 were dissolved in ethanol to give stocks of 10mM.
689 Pentylenetetrazole (PTZ) was dissolved in E3 medium to give a stock of 200mM.
690 SAFit2 and SIB1893 were dissolved in DMSO to give stock concentrations of 10mM
691 and 50mM, respectively. LY354470 was dissolved in water to give a stock
692 concentration of 50mM. Chemical stocks were then diluted into E3 medium
693 containing embryos or larvae, which were then incubated at 28.5^{o}C for the required
694 period of time, before larvae were collected for molecular analysis or analysed for
695 behavioural phenotypes in the Zebrabox .
696
697
698

Electrophysiological analysis of neuronal activity in stxbp1a^{sh438} mutant and sibling larvae

Zebrafish larvae aged 3-4 d.p.f. were anaesthetized in 0.02% tricaine (MS-222, Sigma–Aldrich, UK) and pinned through the notochord onto an electrophysiological recording chamber. After removal of the overlying skin, muscles in one rhabdomere were removed using a sharpened tungsten wire to uncover the spinal cord. The preparation was transferred to a microscope stage and perfused at room temperature (1ml per min, 20–24°C) with an aerated recording solution that contained 15 μM d-tubocurarine (Sigma) to paralyze the preparations, but lacked tricaine. The recording solution contained (in mM) 134 NaCl, 2.9 KCl, 2.1 $CaCl_2$, 1.2 $MgCl_2$, 10 HEPES, and 10 D-glucose, 285 mOsm, pH 7.8. Whole-cell recordings were obtained from large cell-bodied neurons (assumed to be motor neurones, but identity not validated). Patch-clamp pipettes, pulled from borosilicate glass, had resistances of 3.5–5 MΩ. The intracellular solution contained (in mM) 115 K-gluconate, 15 KCl, 2 $NaCl_2$, 10 HEPES, 10 EGTA, 295 mOsm, pH 7.2. Recordings were made in I-clamp mode using an Axopatch 200B amplifier (Molecular Devices, Sunnyvale, CA) and were low-pass filtered at 1 kHz and digitized at 10 kHz.

Light Sheet Imaging of neuronal activity in in stxbp1a^{sh438} mutant and sibling larvae

Adult carriers of both the *stxbp1a^{sh438}* mutation and the *Tg(Xla.Tubb:GCaMP3)^{sh344}* transgene (Bergmann et al., 2018) were crossed to generate transgenic embryos that were either homozygous for the *stxbp1a^{sh438}* mutant allele and immotile, or siblings that were motile. When they were aged 3 d.p.f., transgenic embryos that were motile or immotile were then mounted in 3% agarose in the Zeiss Z.1 Light Sheet microscope and imaged for 5 minutes. Imaging data was processed and

analysed with an algorithm to measure GCaMP3 fluorescence levels within larval brain Z-sections (Bergmann et al., 2018).

Statistical analysis

Statistical analysis and graphics were created in 'R' and Graphpad Prism. Data were tested for equal variance and normality prior to analysis. Statistical significance was tested using *t*-tests or Analysis Of Variance and *post hoc* analysis via pairwise comparisons. Where data under analysis was not normally distributed, significance was determined using the Mann-Whitney test with Sidak's correction. In all graphs, bars represent the mean ± standard error of the mean. * indicates $p<0.05$, ** $p<0.01$, *** $p<0.001$, **** $p<0.0001$.

Acknowledgements

This research was funded by an award to VTC and M Placzek from the UK joint Biotechnology and Biological Sciences Research Council / Economic and Social Research Council Epigenetics Initiative (grant number ES/N000528/1), by a Pilot Grant in Epilepsy to VTC from Epilepsy Research UK (PGE1303), by a Research Grant to VTC and NK from the International Fund raising for Congenital Adrenal Hyperplasia, and by a PhD studentship to DS from the Medical Research Council Discovery Medicine North Doctoral Training Partnership (MR/N013840/1). We thank the zebrafish aquarium staff at the University of Sheffield for fish care and husbandry, the Sheffield Zebrafish Screening Facility for behavioural analysis, and the staff of the University of Sheffield Wolfson Light Microscopy Facility, for light-sheet microscopy, supported by a BBSRC ALERT14 award (BB/M012522/1). We are grateful to Wolf Reik, Felix Krueger, Thomas Stubbs, Ferdinand von Meyenn,

749 Jurriaan Ton and Joost Stassen for advice on methods for methylome analysis, and
750 Anton Nikolaev for help with analysing live imaging data. RAB thanks Declan Ali for
751 training in zebrafish electrophysiology and acknowledges the Biotechnology and
752 Biological Sciences Research Council for research funding (BB/L027690/1).

753

754 **Author Contributions**

755 VTC conceived the study; HE, DS, HEJ, RAB and VTC designed the experiments;
756 HE, DS, HEJ, GW, KB, JPA, RAB and VTC performed the experiments; HE, DS,
757 HEJ, GW, KB, EE, NK, RAB, M Placzek and VTC analysed the experimental results;
758 HE, DS, UE, FS, M Pirooznia and EE performed computational bioinformatic
759 analysis of DNA sequence data; HE, DS, HEJ, NK, RAB, M Placzek and VTC wrote
760 the manuscript. All authors read and approved the final manuscript.

761

762 **Ethics**

763 Animal experimentation: all animal work was performed under licence from the UK
764 Home Office and approved by the University of Sheffield Ethical Review Committee
765 (ASPA Ethical Review Process).

766

767 **Competing Interests**

768 The authors declare that they have no competing interests.

769

770 **Data Availability**

771 Source data for this study are available within the article, its supplementary
772 information files and in the Gene Expression Omnibus under Accession Code
773 GSE120632.

References

Baxendale, S., Holdsworth, C.J., Meza Santoscoy, P.L., Harrison, M.R., Fox, J., Parkin, C.A., Ingham, P.W., and Cunliffe, V.T. (2012). Identification of compounds with anti-convulsant properties in a zebrafish model of epileptic seizures. Dis Model Mech *5*, 773-784.

Bergmann, K., Meza Santoscoy, P., Lygdas, K., Nikolaeva, Y., MacDonald, R.B., Cunliffe, V.T., and Nikolaev, A. (2018). Imaging Neuronal Activity in the Optic Tectum of Late Stage Larval Zebrafish. J Dev Biol *6*.

Bernstein, D.L., Kameswaran, V., Le Lay, J.E., Sheaffer, K.L., and Kaestner, K.H. (2015). The BisPCR(2) method for targeted bisulfite sequencing. Epigenetics Chromatin *8*, 27.

Boyd, P.J., Cunliffe, V.T., Roy, S., and Wood, J.D. (2015). Sonic hedgehog functions upstream of disrupted-in-schizophrenia 1 (disc1): implications for mental illness. Biol Open *4*, 1336-1343.

Cachat, J., Stewart, A., Grossman, L., Gaikwad, S., Kadri, F., Chung, K.M., Wu, N., Wong, K., Roy, S., Suciu, C., *et al.* (2010). Measuring behavioral and endocrine responses to novelty stress in adult zebrafish. Nat Protoc *5*, 1786-1799.

Caporaso, J.G., Kuczynski, J., Stombaugh, J., Bittinger, K., Bushman, F.D., Costello, E.K., Fierer, N., Pena, A.G., Goodrich, J.K., Gordon, J.I., *et al.* (2010). QIIME allows analysis of high-throughput community sequencing data. Nat Methods *7*, 335-336.

Criado-Marrero, M., Rein, T., Binder, E.B., Porter, J.T., Koren, J., 3rd, and Blair, L.J. (2018). Hsp90 and FKBP51: complex regulators of psychiatric diseases. Philosophical transactions of the Royal Society of London Series B, Biological sciences *373*.

Eachus, H., Bright, C., Cunliffe, V.T., Placzek, M., Wood, J.D., and Watt, P.J. (2017). Disrupted-in-Schizophrenia-1 is essential for normal hypothalamic-pituitary-interrenal (HPI) axis function. Human molecular genetics *26*, 1992-2005.

Facchinello, N., Skobo, T., Meneghetti, G., Colletti, E., Dinarello, A., Tiso, N., Costa, R., Gioacchini, G., Carnevali, O., Argenton, F., *et al.* (2017). nr3c1 null mutant zebrafish are viable and reveal DNA-binding-independent activities of the glucocorticoid receptor. Sci Rep *7*, 4371.

Gaali, S., Kirschner, A., Cuboni, S., Hartmann, J., Kozany, C., Balsevich, G., Namendorf, C., Fernandez-Vizarra, P., Sippel, C., Zannas, A.S., *et al.* (2015). Selective inhibitors of the FK506-binding protein 51 by induced fit. Nat Chem Biol *11*, 33-37.

Galat, A. (2013). Functional diversity and pharmacological profiles of the FKBPs and their complexes with small natural ligands. Cell Mol Life Sci *70*, 3243-3275.

Gray, J.D., Kogan, J.F., Marrocco, J., and McEwen, B.S. (2017). Genomic and epigenomic mechanisms of glucocorticoids in the brain. Nat Rev Endocrinol *13*, 661-673.

Griffiths, B.B., Schoonheim, P.J., Ziv, L., Voelker, L., Baier, H., and Gahtan, E. (2012). A zebrafish model of glucocorticoid resistance shows serotonergic modulation of the stress response. Front Behav Neurosci *6*, 68.

Grone, B.P., Marchese, M., Hamling, K.R., Kumar, M.G., Krasniak, C.S., Sicca, F., Santorelli, F.M., Patel, M., and Baraban, S.C. (2016). Epilepsy, Behavioral Abnormalities, and Physiological Comorbidities in Syntaxin-Binding Protein 1 (STXBP1) Mutant Zebrafish. PLoS One *11*, e0151148.

Grossmann, C., Scholz, T., Rochel, M., Bumke-Vogt, C., Oelkers, W., Pfeiffer, A.F., Diederich, S., and Bahr, V. (2004). Transactivation via the human glucocorticoid and mineralocorticoid receptor by therapeutically used steroids in CV-1 cells: a comparison of their glucocorticoid and mineralocorticoid properties. Eur J Endocrinol *151*, 397-406.

Guo, W., Fiziev, P., Yan, W., Cokus, S., Sun, X., Zhang, M.Q., Chen, P.Y., and Pellegrini, M. (2013). BS-Seeker2: a versatile aligning pipeline for bisulfite sequencing data. BMC Genomics *14*, 774.

Hwang, W.Y., Fu, Y., Reyon, D., Maeder, M.L., Tsai, S.Q., Sander, J.D., Peterson, R.T., Yeh, J.R., and Joung, J.K. (2013). Efficient genome editing in zebrafish using a CRISPR-Cas system. Nat Biotechnol *31*, 227-229.

Kadmiel, M., and Cidlowski, J.A. (2013). Glucocorticoid receptor signaling in health and disease. Trends Pharmacol Sci *34*, 518-530.

Kimmel, C.B., Ballard, W.W., Kimmel, S.R., Ullmann, B., and Schilling, T.F. (1995). Stages of embryonic development of the zebrafish. Dev Dyn *203*, 253-310.

Klengel, T., Mehta, D., Anacker, C., Rex-Haffner, M., Pruessner, J.C., Pariante, C.M., Pace, T.W., Mercer, K.B., Mayberg, H.S., Bradley, B.*, et al.* (2013). Allele-specific FKBP5 DNA demethylation mediates gene-childhood trauma interactions. Nature neuroscience *16*, 33-41.

Krueger, F., and Andrews, S.R. (2011). Bismark: a flexible aligner and methylation caller for Bisulfite-Seq applications. Bioinformatics *27*, 1571-1572.

Li, L.C., and Dahiya, R. (2002). MethPrimer: designing primers for methylation PCRs. Bioinformatics *18*, 1427-1431.

Ludewig, S., and Korte, M. (2016). Novel Insights into the Physiological Function of the APP (Gene) Family and Its Proteolytic Fragments in Synaptic Plasticity. Front Mol Neurosci *9*, 161.

Matsui, M., Fowler, J.H., and Walling, L.L. (2006). Leucine aminopeptidases: diversity in structure and function. Biol Chem *387*, 1535-1544.

McEwen, B.S. (2012). Brain on stress: how the social environment gets under the skin. Proc Natl Acad Sci U S A *109 Suppl 2*, 17180-17185.

McEwen, B.S., and Wingfield, J.C. (2010). What is in a name? Integrating homeostasis, allostasis and stress. Horm Behav *57*, 105-111.

Mi, H., Muruganujan, A., Casagrande, J.T., and Thomas, P.D. (2013). Large-scale gene function analysis with the PANTHER classification system. Nat Protoc *8*, 1551-1566.

Mifsud, K.R., and Reul, J. (2018). Mineralocorticoid and glucocorticoid receptor-mediated control of genomic responses to stress in the brain. Stress *21*, 389-402.

Nasca, C., Bigio, B., Zelli, D., Nicoletti, F., and McEwen, B.S. (2015a). Mind the gap: glucocorticoids modulate hippocampal glutamate tone underlying individual differences in stress susceptibility. Mol Psychiatry *20*, 755-763.

Nasca, C., Zelli, D., Bigio, B., Piccinin, S., Scaccianoce, S., Nistico, R., and McEwen, B.S. (2015b). Stress dynamically regulates behavior and glutamatergic gene expression in hippocampus by opening a window of epigenetic plasticity. Proc Natl Acad Sci U S A *112*, 14960-14965.

Popoli, M., Yan, Z., McEwen, B.S., and Sanacora, G. (2011). The stressed synapse: the impact of stress and glucocorticoids on glutamate transmission. Nat Rev Neurosci *13*, 22-37.

Sacta, M.A., Chinenov, Y., and Rogatsky, I. (2016). Glucocorticoid Signaling: An Update from a Genomic Perspective. Annu Rev Physiol *78*, 155-180.

Sander, J.D., Maeder, M.L., Reyon, D., Voytas, D.F., Joung, J.K., and Dobbs, D. (2010). ZiFiT (Zinc Finger Targeter): an updated zinc finger engineering tool. Nucleic Acids Res *38*, W462-468.

Schauenburg, L., Liebsch, F., Eravci, M., Mayer, M.C., Weise, C., and Multhaup, G. (2018). APLP1 is endoproteolytically cleaved by gamma-secretase without previous ectodomain shedding. Sci Rep *8*, 1916.

Schilling, S., Mehr, A., Ludewig, S., Stephan, J., Zimmermann, M., August, A., Strecker, P., Korte, M., Koo, E.H., Muller, U.C., *et al.* (2017). APLP1 Is a Synaptic Cell Adhesion Molecule, Supporting Maintenance of Dendritic Spines and Basal Synaptic Transmission. The Journal of neuroscience : the official journal of the Society for Neuroscience *37*, 5345-5365.

Treccani, G., Musazzi, L., Perego, C., Milanese, M., Nava, N., Bonifacino, T., Lamanna, J., Malgaroli, A., Drago, F., Racagni, G., *et al.* (2014). Stress and corticosterone increase the readily releasable pool of glutamate vesicles in synaptic terminals of prefrontal and frontal cortex. Mol Psychiatry *19*, 433-443.

Wochnik, G.M., Ruegg, J., Abel, G.A., Schmidt, U., Holsboer, F., and Rein, T. (2005). FK506-binding proteins 51 and 52 differentially regulate dynein interaction and nuclear translocation of the glucocorticoid receptor in mammalian cells. J Biol Chem *280*, 4609-4616.

Yeh, C.M., Glock, M., and Ryu, S. (2013). An optimized whole-body cortisol quantification method for assessing stress levels in larval zebrafish. PLoS One *8*, e79406.

Zannas, A.S., and Binder, E.B. (2014). Gene-environment interactions at the FKBP5 locus: sensitive periods, mechanisms and pleiotropism. Genes Brain Behav *13*, 25-37.

Zannas, A.S., and Chrousos, G.P. (2017). Epigenetic programming by stress and glucocorticoids along the human lifespan. Mol Psychiatry *22*, 640-646.

Zannas, A.S., Wiechmann, T., Gassen, N.C., and Binder, E.B. (2016). Gene-Stress-Epigenetic Regulation of FKBP5: Clinical and Translational Implications. Neuropsychopharmacology : official publication of the American College of Neuropsychopharmacology *41*, 261-274.

Ziv, L., Muto, A., Schoonheim, P.J., Meijsing, S.H., Strasser, D., Ingraham, H.A., Schaaf, M.J., Yamamoto, K.R., and Baier, H. (2013). An affective disorder in zebrafish with mutation of the glucocorticoid receptor. Mol Psychiatry *18*, 681-691.

.

Figure Legends

Figure 1

The Glucocorticoid Receptor (GR) regulates behaviour and whole body cortisol levels in larval and adult zebrafish.

(A) Shoaling analysis of 5 d.p.f. larvae under baseline (control) and stressed (NaCl) conditions. Swimming speed of wild-type shoals (21 larvae per shoal) is reduced under stress, whilst *gr*^{s357} mutant larvae swim more slowly than wild-type larvae under baseline conditions, and swim speed is not affected by saline stress. Values are expressed as means +/- s.e.m. A two-way ANOVA identified genotype:treatment interactions, F=14.41, d.f.=1, 20, p=0.001). N = 6 each group. * indicates statistical differences in Tukey post-hoc analysis, * $p < 0.05$, ** $p < 0.01$, *** $p < 0.001$.

(B) The Nearest Neighbour Distance (NND) of wild-type shoals increases under saline stress, whilst *gr*^{s357} mutant shoals exhibit a higher NND than wild-type larvae, both at baseline and under conditions of saline stress. Values are expressed as means +/- s.e.m. A two-way ANOVA identified genotype: treatment interactions, F=8.09, d.f.=1, 20, p=0.01). N = 6 shoals (21 larvae per shoal) each group. * indicates statistical differences in Tukey post-hoc analysis, * $p < 0.05$, ** $p < 0.01$.

(C-E) Behavioural analysis of adult fish in the open field test reveals that *gr*^{s357} mutants show (C) increased duration of freezing (*t*-test, *t*=-3.57, d.f.=15.33, p=0.003), (D) increased duration of slow swimming (*t*-test, *t*=-2.94, d.f.=13.11, p=0.011), and (E) decreased thigmotaxis (*t*-test, *t*=2.47, d.f.=12.86, p=0.028), in comparison to wild-type siblings. Values are expressed as means +/- s.e.m. N = 9 each group. * $p < 0.05$, ** $p < 0.01$.

(F-H) Behavioural analysis of adult fish in the light-dark scototaxis test reveals that (F) whilst wild-type adults display a significant initial preference for the light part of the tank, *gr*^{s357} mutants show no preference for either the light or the dark areas (repeated measures ANOVA, Genotype: time interaction: F=4.60, d.f.=1,15, p=0.048, N=7-8 each genotype). Representative traces of (G) wild-type and (H) *gr*^{s357} swimming in minute 1 of the light-dark scototaxis test. Values are expressed as means +/- s.e.m., * indicates statistical differences in Tukey post-hoc analysis, * p < 0.05, ** p < 0.01, *** p < 0.001.

(I-J) Behavioural analysis of adult fish in the novel tank diving test. (I) Adult *gr*^{s357}mutant fish swim more slowly than wild-type adults (ANOVA with repeated measures: significant effect of genotype (F=7.38, df=1,30, p=0.011, N=9 each genotype). (J) Adult *gr*^{s357}mutant fish are less exploratory than wild-type adults, exhibiting fewer entries to the upper compartment of the novel tank than wild-types. Values are expressed as means +/- s.e.m. A two-way ANOVA identified significant genotype:time interactions (F=6.57, df=1,30, p=0.016, N=9 each genotype), * p < 0.05, ** p < 0.01, *** p < 0.001.

(K) *gr*^{s357} mutant adult males have elevated whole body cortisol levels compared to their wild-type siblings (*t*-test, *t*=-3.26, d.f.=4.05, p=0.03). Values are expressed as means +/- s.e.m. N= 5 each.

(L) 5 d.p.f. *gr*^{s357} mutant larvae have elevated whole body cortisol levels compared to wild type larvae (*t*-test, *t*=-3.30, d.f.=13.31, p=0.006). Values are expressed as means +/- s.e.m. N= 12 each. * indicates statistical differences in Tukey post-hoc analysis, * p < 0.05, ** p < 0.01.

Figure 1 – Source data 1. Source data for analysis of swimming speed and Nearest Neighbour Distances of wild-type and *gr*^{s357} mutant larvae presented in Figures 1A and 1B.

Figure 1 – Source data 2. Source data for analysis of freezing duration, slow swim duration and thigmotaxis of wild-type and *gr*^{s357} mutant adult zebrafish presented in Figures 1C, 1D and 1E.

Figure 1 – Source data 3. Source data for analysis of scototaxis behavior of wild-type and *gr*^{s357} mutant adult zebrafish presented in Figure 1F.

Figure 1 – Source data 4. Source data for analysis of swimming speed and exploratory behaviour of wild-type and *gr*^{s357} mutant adult zebrafish in the novel tank diving test as presented in Figures 1I and 1J.

Figure 1 – Source data 5. Source data for the analysis of whole body cortisol levels in wild-type and *gr*^{s357} mutant adult zebrafish presented in Figure 1K.

Figure 1 – Source data 6. Source data for the analysis of whole body cortisol levels in wild-type and *gr*^{s357} mutant larval zebrafish presented in Figure 1L.

Figure 2

Identification of Glucocorticoid Receptor-regulated DNA methylation sites in the adult brain methylome

To identify GR-sensitive, differentially methylated regions (GR-DMRs) within the zebrafish genome, the whole brain methylomes of two wild-type adult and two *gr*^{s357} mutant males aged 13 months were completely sequenced and compared. A total of 470,880,704 reads were obtained, of which 95.2% were high quality reads, and 49.3% of these were mapped to the GRCz10 release 85 zebrafish reference genome. 99.15% of the genome was successfully bisulfite converted. Average coverage for all CpGs across the genome was 3.475. Average methylation level across the genome was 84.24% for wild types and 83.97% for *gr*^{s357} mutants.

(A) DeepTools (v3.1.3) Heatmap showing the distribution of methylated CpGs within and flanking gene bodies in wild-type and *gr*^{s357} mutant adult brain samples, covering the region from 5kb upstream of the Transcription Start site (TSS), to 5kb downstream of the Transcription Termination Site (TTS), for the 1448 genes for which there was >95% coverage of CpGs within the plotted region, in the adult brain samples analysed by WGBS. Deeper blue corresponds to a higher level of methylation. In both wild-type and *gr*^{s357} mutant samples, gene bodies are typically highly methylated and promoters exhibit reduced or absent methylation, confirming that the global genomic DNA methylation patterns in the zebrafish brain samples analysed were similar to those described in other vertebrates.

(B) Histogram showing the frequency distribution of GR-DMRs identified by WGBS according to number of CpGs within the DMR. 171 of the 249 DMRs identified in the WGBS analysis comprised a single CpG, with an additional 55 DMRs comprising two CpGs, and the remaining 23 containing 3 or more clustered CpGs.

(C) Plot of the number of CpGs within DMRs against the AreaStat measure of differential methylation (mean +/- s.e.m.). Negative values indicate DMRs are hypomethylated in the *gr*^{s357} mutant adult male brain compared to wild-type; positive values indicate DMRs are hypermethylated in the *gr*^{s357} mutant adult male brain compared to wild-type.

Figure 2 – Source data 1

Differentially methylated regions identified in adult GR mutant brains using WGBS.

The bsseq software package was used to identify 249 genomic loci exhibiting differential methylation in the brains of adult *gr*^{s357} mutant and wild-type sibling males. N = 2 animals per genotype. 142 DMRs (57%) exhibited hypermethylation of CpGs within the DMR in mutant compared to wild type brain samples. For the remaining 107 DMRs (43%), the CpG(s) were hypomethylated in the *gr*^{s357} mutant compared to wild-type brain samples. Each DMR was annotated with information about their proximity to transcription units. 141 of these DMRs were located within known genes (i.e. present in known exons or introns), with the remaining 109 DMRs being located either upstream or downstream of known genes.

Abbreviations: Chr – chromosome; Start – start position of DMR; End – end position of DMR; idxStart, idxEnd, Cluster – 'Internal use'; N – Number of CpGs in DMR; Width – Width of DMR; Invdensity – Average length per locus; Areastat – sum of the *t*-statistics in each CpG (This is the area of the DMR, weighted by the number of CpGs rather than by genomic length); maxStat – max *t*-statistic; meanDiff – The mean difference in methylation level; the difference between group1.mean and group2.mean ; Group1.mean – The mean methylation level across samples and loci

in 'group1' :Mutant; Group2.mean – The mean methylation level across samples and loci in 'group2' :wild type; Tstat.sd – standard deviation of *t*-statistics; Direction - either 'hyper' or 'hypo' methylated.

Figure 2 – Figure supplement 1

Gene Ontology (GO) analysis of GR-DMR associated genes in PANTHER.

In order to gain insight into the downstream biological pathways that might be regulated by GR, Gene Ontology (GO) analysis using PANTHER was performed for genes either lying adjacent to a DMR or within which a DMRs is located (Mi et al., 2013). The PANTHER Over-representation Test identifed 14 GO terms within the Biological Process category that are significantly associated (False Discovery Rate < 0.05) with DMR-linked genes, showing a fold-enrichment of between 1.37 and 3.18 (Supplementary Table 1). Many of these terms are broadly relevant to the known function of GR as a mediator of signalling pathway activity, suggesting that some of identified DMRs could be involved in transcriptional regulation of GR target genes with functions in the CNS.

Figure 2 – Figure supplement 2

BisPCR^2 targeted bisulfite sequencing of DMRs identified via WGBS.

The mean number of sequence reads was calculated for each of the 11 DMRs analysed by BisPCR^2 in the 10 wild-type and 10 *gr*^{s357} mutant adult male brain samples, indicating the gene name (first column), the genomic location (second column) and mean number of amplicon reads in wild-type and *gr*^{s357} mutant animals.

Figure 2 – Figure supplement 3

Differential methylation of individual CpGs in the fkbp5, npepl1 and aplp1 GR-DMRs. Methylation levels at each CpG were compared in 10 wild-type and 10 *gr*^{s357} mutant adult male brain samples for the *fkbp5, npepl1* and *aplp1* DMRs. A Mann-Whitney test with Sidak correction for multiple comparisons identified significantly differentially methylated CpGs. * p<0.05, ** p<0.01, *** p<0.001 (n.s., not significant).

Figure 2 – Figure supplement 4

BiSPCR^2 analysis of DNA methylation within a subset of GR-DMRs identified by WGBS

(A-H) The percentage methylation of individual CpGs within a subset of high-ranking GR-DMRs identified in the WGBS analysis, was determined using the BisPCR^2 technique (Bernstein et al., 2015) in the brains of 10 wild-type and 10 *gr*^{s357} mutant adult males aged 15 months. In addition to *fkbp5*, *npepl1* and *aplp1*, DMRs associated with the following genes were analysed: (A) *foxred2*, (B) *lpar6/ece2b*, (C) *chrm2a*, (D) *npy2rl*, (E) *stxbp5l*, (F) *dpp6a*, (G) *gna14*, (H) *ptger1c*. Histograms show mean percentage methylation +/- s.e.m. (n = 10 per genotype) in wild-type and *gr*^{s357} mutant adult brains. An overall mean coverage of 4093 reads per amplicon was obtained, averaged across all samples subjected to BisPCR^2 analysis. Statistical analysis was performed using Mann-Whitney tests with Sidak correction, * p<0.05, ** p<0.01, *** p<0.001. Details of the mean number of reads for each DMR are presented in Supplementary Table 2.

Figure 2 – Figure supplement 4 – Source data 1. Source data for the *BiSPCR^2 analysis of DNA methylation within a subset of GR-DMRs identified by WGBS*

in wild-type and *gr*^{s357} mutant zebrafish.

Figure 3

The Glucocorticoid Receptor regulates DNA methylation and transcription of* fkbp5 *in zebrafish

(A) The percentage methylation of each of the 4 CpGs within the *fkbp5* GR-DMR identified in the WGBS analysis was determined using the BisPCR^2 technique, in the brains of 10 wild-type (GR WT) and 10 *gr*^{s357} homozygous mutant (GR mutant) adult males (on the y-axis, 1.0 = 100%). Numbers on the *x*-axis indicate nucleotide position on chromosome 6 (GRCz10 release 85). Histogram shows mean percentage methylation +/- s.e.m. for each CpG in wild-type and *gr*^{s357} mutant adult brains. A mean coverage of 2813 and 3167 reads per sample was obtained for the *fkbp5* amplicon in wild-type and *gr*^{s357} mutant brains, respectively. Significant differentially methylated CpGs were identified using the Mann-Whitney test with Sidak correction for multiple comparisons. ** p<0.01, *** p<0.001.

(B) qRT-PCR analysis of *fkbp5* transcript abundance in brains of wild-type and gr^{s357} homozygous mutant adult males. Transcript abundance was normalized to levels of beta actin transcription, values are displayed as means +/- s.e.m., n = 7. Statistical analysis by *t*-test revealed significantly decreased *fkbp5 transcript* abundance in the brains of *gr*^{s357} mutant compared to wild-type adult males. **** p<0.0001.

(C) BisPCR^2 analysis of DNA methylation at the 4 CpG dinucleotides within the *fkbp5* GR-DMR in wild-type and *gr*^{s357} homozygous mutant 256-cell stage blastulae. Histograms show mean percentage methylation +/- s.e.m. (12 pools of 50 blastulae

per pool). A Mann-Whitney test revealed no statistically significant differences in mean percentage methylation at any of the 4 CpGs within the GR-DMR.

(D) BisPCR^2 analysis of DNA methylation at the 4 CpG dinucleotides within the *fkbp5* GR-DMR in dissected head tissue of individual wild-type and *gr*^{s357} homozygous mutant larvae, maintained overnight for 16 hours until they reached 5 d.p.f., in the presence (GR WT-BM, GR mutant-BM) or absence (GR WT, GR mutant) of 100μM betamethasone. Histograms show mean percentage methylation +/- s.e.m. (n = 24 larvae per genotype/treatment group). A Mann-Whitney test with Sidak correction for multiple comparisons revealed statistically significant differences in mean percentage methylation at CpGs: 6: 41099291, 6: 41099420 and 6: 41099447. * p<0.05, *** p<0.001.

(E) qRT-PCR analysis of *fkbp5* mRNA levels in 3 d.p.f. and 5 d.p.f. wild-type and *gr*^{s357} homozygous mutant larvae maintained in E3 medium only (untreated), E3 medium containing 100μM betamethasone for 2 hours. Histograms show mean transcript abundance +/- s.e.m relative to *β-actin,* normalized to the wild-type control group (n = 6 pools of 20 larvae per genotype/treatment group). A two-way ANOVA identified statistically significant differences in transcript abundance: ** p<0.01, *** p<0.001.

(F) Whole mount *in situ* hybridisation analysis of *fkbp5* transcript levels in 5 d.p.f. wild-type and *gr*^{s357} (*nr3c1 -/-*) mutant larvae reveals weak *fkbp5* expression in untreated wild-type larvae, strong *fkbp5* expression in wild-type larvae treated with 100μM betamethasone for 2 hours, and a complete absence of *fkbp5* transcripts in both untreated and betamethasone-treated *gr*^{s357}mutants. Images are typical of each genotype / treatment group, ~ 30 larvae per group.

Figure 3 – Source data 1. Source data for the analysis of DNA methylation at the *fkbp5* GR-DMR in wild-type and *gr*^{s357} mutant zebrafish presented in Figures 3A, 3C and 3D.

Figure 3 – Source data 2. Source data for the analysis of *fkbp5* transcript abundance in wild-type and *gr*^{s357} mutant zebrafish presented in Figures 3B and 3E.

Figure 3 – Figure supplement 1

The Glucocorticoid Receptor regulates DNA methylation and transcription of npepl1 in the zebrafish adult brain.

(A) The percentage methylation of each of the 5 CpGs within the *npepl1* GR-DMR identified in the WGBS analysis was determined using the BisPCR^2 technique, in the brains of 10 wild-type (GR WT) and 10 *gr*^{s357} homozygous mutant (GR mutant) adult males (on the y-axis, 1.0 = 100%). Numbers on the *x*-axis indicate nucleotide position on chromosome 6 (GRCz10 release 85). Histogram shows mean percentage methylation +/- s.e.m. for each CpG in wild-type and *gr*^{s357} mutant adult brains. A mean coverage of 3453 and 2443 reads per sample was obtained for the *npepl1* amplicon in wild-type and *gr*^{s357} mutant brains, respectively. Significant differentially methylated CpGs were identified using the Mann-Whitney test with Sidak correction for multiple comparisons. * $p<0.05$.

(B) qRT-PCR analysis of GR-DMR-associated *npepl1* transcript abundance in wild-type and gr^{s357} mutant adult male brains. Transcript abundance was normalized to levels of beta actin transcription, values are displayed as means +/- s.e.m., n = 7. Statistical analysis by *t*-test revealed a modest but significant reduction in *npepl1*

transcript abundance in the brains of *gr*^{s357} mutant compared to wild-type adult males. *** p<0.001.

Figure 3 – Figure supplement 1 – Source data 1

Source data for the analysis of DNA methylation at the *npepl1* GR-DMR and *npepl1* transcript abundance, in wild-type and *gr*^{s357} mutant zebrafish, as presented in Figures Figure 3-supplement 1A and 1B, respectively.

Figure 4

The Glucocorticoid Receptor regulates DNA methylation and transcription of aplp1 in zebrafish

(A) The percentage methylation of each of the 6 CpGs within the *aplp1* GR-DMR identified in the WGBS analysis was determined using the BisPCR^2 technique in the brains of 10 wild-type (GR WT) and 10 *gr*^{s357} homozygous mutant (GR mutant) adult males. Numbers on the *x*-axis indicate nucleotide position on chromosome 15 (GRCz10 release 85). Histogram shows mean percentage methylation +/- s.e.m. for each CpG in wild-type and *gr*^{s357} mutant adult brains. On average, a mean coverage of 7881 and 7125 reads per sample were obtained for the *aplp1* amplicon in wild-type and *gr*^{s357} mutant brains, respectively. Significant differentially methylated CpGs were identified using the Mann-Whitney test with Sidak correction for multiple comparisons. * p<0.05, ** p<0.01, *** p<0.001.

(B) qRT-PCR analysis of *aplp1* mRNA abundance in the brains of wild-type and gr^{s357} homozygous mutant adult males. mRNA abundance was normalized to levels of beta actin transcripts, values are displayed as means +/- s.e.m., n = 7. Statistical

analysis by *t*-test revealed significantly increased *aplp1* transcript abundance in the brains of *gr*^{s357} mutant compared to wild-type adult males. ** p<0.01, *** p<0.001, **** p<0.0001.

(C) BisPCR^2 analysis of DNA methylation within the *aplp1* GR-DMR in wild-type and *gr*^{s357} homozygous mutant 256-cell stage blastulae. Histograms show mean percentage methylation +/- s.e.m. (12 pools of 50 blastulae per pool). A Mann-Whitney test revealed no statistically significant differences in mean percentage methylation at any of the 6 CpGs within the GR-DMR.

(D) BisPCR^2 analysis of DNA methylation at the 6 CpG dinucleotides within the *aplp1* GR-DMR in dissected head tissue of individual 5 d.p.f. wild-type and *gr*^{s357} homozygous mutant larvae, maintained overnight for 16 hours until they reached 5 d.p.f., in the presence (GR WT-BM, GR mutant-BM) or absence (GR WT, GR mutant) of 100μM betamethasone, prior to DNA extraction. Histograms show mean percentage methylation +/- s.e.m. (n = 24 larvae per genotype/treatment group). A Mann-Whitney test with Sidak correction for multiple comparisons revealed no statistically significant differences in mean percentage methylation at any of the six CpGs within the GR-DMR.

(E) qRT-PCR analysis of *aplp1* mRNA levels in 3 d.p.f. and 5 d.p.f. wild-type and *gr*^{s357} homozygous mutant larvae maintained in E3 medium only (untreated), or E3 medium containing 100μM betamethasone for 2 hours. Histograms show mean transcript abundance +/- s.e.m relative to *β-actin,* normalized to the wild-type control group (n = 6 pools of 20 larvae per genotype/treatment group). A two-way ANOVA identified statistically significant differences in transcript abundance: * p<0.05, *** p<0.001, **** p<0.0001.

(F) Whole mount *in situ* hybridisation analysis of *aplp1* transcript levels in 5 d.p.f. wild-type and *gr*^{s357} mutant (*nr3c1 -/-*) larvae maintained in E3 medium only (untreated), E3 medium containing 100μM betamethasone for 2 hours reveals modest *aplp1* expression in the untreated wild-type and *gr*^{s357} mutant larval brain, and a considerable increase in transcript abundance in betamethasone-treated wild-type larvae, which was not observed in betamethasone-treated *gr*^{s357} mutant larvae. Images are typical of each genotype / treatment group, ~ 30 larvae per group.

Figure 4 – Source data 1. Source data for the analysis of DNA methylation at the *aplp1* GR-DMR in wild-type and *gr*^{s357} mutant zebrafish presented in Figures 4A, 4C and 4D.

Figure 4 – Source data 2. Source data for the analysis of *aplp1* transcript abundance in wild-type and *gr*^{s357} mutant zebrafish presented in Figures 4B and 4E.

Figure 5

Small molecule inhibitors of FKBP5 function enhance GR-dependent glucocorticoid-induced transcription of fkbp5 mRNA but have no effect on GR-dependent, glucocorticoid-induced transcription of aplp1.

(A, B) Triplicate pools of wild-type (GR WT) and *gr*^{s357} homozygous mutant (GR mutant) larvae (20 larvae per pool, 4 d.p.f.) were exposed to E3 medium only or E3 medium containing 1μM FK506 for one hour before being transferred to E3 medium containing 0, 5, 10, 20, 50 or 100μM betamethasone with or without 1μM FK506, and incubated for a further two hours. RNA was then extracted and subjected to qRT-

PCR analysis to quantify abundance of (A) *fkbp5* and (B) *aplp1* mRNAs, normalized to levels of beta actin mRNA. Values are expressed as means +/- s.e.m. A two-way ANOVA identified statistically significant differences in transcript abundance: **** p<0.0001. The presence of 1μM FK506 elicited a betamethasone concentration-dependent increase in *fkbp5* transcript abundance, but did not affect the betamethasone concentration-dependent abundance of *aplp1* transcripts. (C, D) Triplicate pools of wild-type and *gr*^{s357} homozygous mutant larvae (20 larvae per pool, 4 d.p.f.) were exposed to E3 medium only or E3 medium containing 0.1μM SAFit2 for one hour before being transferred to E3 medium containing 0, 5, 10, 20, 50 or 100μM betamethasone with or without 0.1μM SAFit2, and incubated for a further two hours. RNA was then extracted and subjected to qRT-PCR analysis to quantify abundance of (C) *fkbp5* and (D) *aplp1* transcripts, normalized to levels of beta actin mRNA. Values are expressed as means +/- s.e.m. A two-way ANOVA identified statistically significant differences in transcript abundance: * p<0.05, *** p<0.001, **** p<0.0001. The presence of 0.1μM SAFit2 elicited a betamethasone concentration-dependent increase in *fkbp5* transcript abundance but did not affect the betamethasone concentration-dependent abundance of *aplp1* transcripts.

Figure 5 – Source data 1. Source data for the analysis of glucocorticoid-induced transcription of *fkbp5* and *aplp1* in wild-type and *gr*^{s357} mutant zebrafish larvae in the presence or absence of FKBP5 protein inhibitors, as presented in Figures 5A, 5B, 5C and 5D.

Figure 6

The synaptic vesicle docking protein, Syntaxin Binding Protein 1A (Stxbp1a), is required for neural activity in the larval zebrafish brain.

(A) Whole-mount *in situ* hybridisation analysis of *stxbp1a* transcript distribution in wild-type zebrafish embryos and larvae at 1 d.p.f (n=22), 2 d.p.f. (n=14) and 3 d.p.f. (n=23). Dorsal views of embryonic and larval heads. *stxbp1a* is expressed specifically in the developing brain and spinal cord, and also in specific layers of retinal cells in 3 d.p.f. larvae.

(B) Nucleotide sequences at the Exon 8 / Intron 8-9 boundary within the zebrafish *stxbp1a* gene before and after targeted mutagenesis by CRISPR/Cas9. Underlined purple and green nucleotides in the wild-type *stxbp1a* sequence are deleted in the *stxbp1a*^{sh438} mutant allele and replaced with a shorter sequence of nucleotides in red. The mutation removes the Exon 8 / Intron 8-9 splice donor site, extending the open reading frame into Intron 8-9 that is terminated prematurely.

(C) Homozygosity for a loss of function mutation in *stxbp1a* abolishes baseline locomotor activity and convulsive locomotor behaviour in 3 d.p.f. larvae exposed to 5mM Pentylenetetrazole (PTZ), a chemical convulsant. Homozygous *stxbp1a* mutants carrying two copies of the *sh438* allele (Mutant) are completely immotile whereas sibling larvae (WT, includes both phenotypically wild-type *stxbp1a*^{sh438} heterozygotes and homozygous wild-type larvae) exhibit modest baseline locomotor movements and robust locomotor activity when exposed to 5mM PTZ. Values are expressed as means +/- s.e.m. A two-way ANOVA reveals a significant treatment:genotype interaction. F=22.8, d.f.=1,44, p=<0.0001, N=8-15, *** p<0.0001 compared to all groups in Tukey post-hoc analysis.

(D) Electrophysiological patch clamp analysis of individual spinal neurones from 4 d.p.f. phenotypically wild-type sibling (left column, n= 1) and *stxbp1a*^{sh438} homozygous mutant (right column, n = 3) larvae. Top row: examples of baseline neuronal firing in untreated larvae; middle row: examples of convulsant-induced neuronal firing in PTZ-treated larvae; bottom row: neuronal firing induced by current injection into patch-clamped neurons. Spinal neurones of sibling larvae exhibited baseline firing (top left), which was increased by PTZ treatment (middle left), in contrast to neurones of *stxbp1a*^{sh438} homozygous mutant larvae, which exhibited negligible neuronal firing both in the presence (middle right) and absence (top right) of PTZ, although current injection was able to bypass the need for synaptic neurotransmission and elicit neuronal firing in both sibling (bottom left) and *stxbp1a*^{sh438} mutant (bottom right) larvae.

(E) Plots of fluorescence of *Tg(Xla.Tubb:GCaMP3)*^{sh344} –derived GCaMP3 calcium reporter over time (Bergmann et al., 2018) in the presence and absence of *stxbp1a* function. 3 d.p.f. transgenic larvae that were either phenotypically wild-type sibling (motile) or homozygous for the *stxbp1a*^{sh438} mutant allele (immotile) were imaged for a period of 5 minutes on a Zeiss Light sheet microscope. Imaging data was processed and analysed with an in-house algorithm to measure GCaMP3 fluorescence levels within the brain over the 5 minute time period. Data is plotted to show GCaMP3 fluorescence intensity of an equivalent z-slice over time for each imaged sibling (n=6) and homozygous *stxbp1a*^{sh438} mutant (n=5) larval brain. See Figure 6-video 1 and Figure 6-video 2 for examples of imaged sibling and homozygous *stxbp1a*^{sh438} mutant larvae, respectively.

(F) Whole-mount *in situ* hybridisation analysis of neuronal immediate-early gene *cfos* transcription pattern in the brain of 3 d.p.f. *stxbp1a*^{sh438} homozygous mutant (right

column) and phenotypically wild-type sibling (left column) larvae cultured in E3 medium only (top row) or E3 medium containing 20mM PTZ convulsant agent (bottom row). An extensive domain of robust PTZ-induced transcription of *cfos* by PTZ is evident in the brain of siblings (n=17), whereas only a small domain of *stxbp1a*-independent, PTZ-induced transcription of *cfos* is visible in the telencephalon of *stxbp1a*^{sh438} homozygous mutant larvae (n=6), where the paralogue of *stxbp1a, stxbp1b,* is specifically expressed (Grone et al., 2016). No *cfos* transcripts were detectable in untreated sibling (n=16) or *stxbp1a*^{sh438} homozygous mutant larvae (n=4).

Figure 6 – Source data 1. Source data for analysis of locomotor movement by wild-type sibling and homozygous *stxbp1a*^{sh438} mutant larvae in the presence and absence of PTZ, as presented in Figure 6C.

Figure 6 – video 1. Example video recording of GCaMP3 fluorescence in brain of 3 d.p.f. wild-type sibling *Tg(Xla.Tubb:GCaMP3)*^{sh344} transgenic larva, as analysed in Figure 6E.

Figure 6 – video 2. Example video recording of GCaMP3 fluorescence in brain of 3 d.p.f. homozygous *stxbp1a*^{sh438} mutant *Tg(Xla.Tubb:GCaMP3)*^{sh344} transgenic larva, as analysed in Figure 6E.

Figure 7

stxbp1a acts downstream of glucocorticoid signalling to facilitate transcription of _aplp1_ but not _fkbp5_, and has no impact on DNA methylation at either the _aplp1_ or _fkbp5_ GR-DMRs in larval head tissue.

(A, B) Triplicate pools of 4 d.p.f. sibling (Stxbp1a sibling) and *stxbp1a*^{sh438} homozygous mutant (Stxbp1a -/-) larvae (20 larvae per pool) were exposed to E3 medium only or E3 containing 0.1μM SAFit2 for one hour before being transferred to E3 medium containing 0, 5, 10, 20, 50 or 100μM betamethasone with or without 0.1μM SAFit2, and incubated for a further two hours. RNA was then extracted from each pool and subjected to qRT-PCR analysis to quantify abundance of (A) *aplp1* and (B) *fkbp5* transcripts, normalized to levels of beta actin mRNA. Values are expressed as means +/- s.e.m. A two-way ANOVA identified statistically significant differences in transcript abundance: ** p<0.01, *** p<0.001, **** p<0.0001. The presence of 0.1μM SAFit2 elicited a betamethasone concentration-dependent increase in *fkbp5* transcript abundance but did not affect the betamethasone concentration-dependent abundance of *aplp1* transcripts. Thus in (A), *stxbp1a* is required for betamethasone-mediated induction of *aplp1* transcription, which is strictly insensitive to the Fkbp5 inhibitor, SAFit2. In (B), *stxbp1a* is dispensable for the betamethasone-mediated induction of *fkbp5* transcription, which is greatly enhanced by the Fkbp5 inhibitor, SAFit2, in the presence or absence of *stxbp1a* function.

(C) BisPCR^2 analysis of DNA methylation at the *aplp1* GR-DMR in dissected head tissue of 4 d.p.f. betamethasone-treated and untreated wild-type sibling and *stxbp1a*^{sh438} homozygous mutant larvae (n=24 individual larval heads per genotype/treatment group). Histogram shows mean percentage methylation for each

CpG +/- s.e.m. A Mann-Whitney test revealed no statistically significant differences in mean percentage methylation at any of the 6 CpGs within the GR-DMR.

(D) DNA methylation analysis at the *fkbp5* GR-DMR in 4 d.p.f. betamethasone-treated and untreated wild-type sibling and *stxbp1a*^{sh438} homozygous mutant larvae (n=24 individual larval heads per genotype/treatment group). Histogram shows mean percentage methylation for each CpG +/- s.e.m. Significant differentially methylated CpGs were identified using the Mann-Whitney test with Sidak correction for multiple comparisons. ** p<0.01, *** p<0.001.

(E, F) Five pools of 4 d.p.f. wild-type and homozygous *gr*^{s357} mutant larvae (20 larvae per pool) were exposed to E3 medium only or E3 medium containing 20mM PTZ for 90 minutes. RNA was then extracted from whole larvae and subjected to qRT-PCR to quantify (E) *fkbp5* transcript abundance, and (F) *aplp1* transcript abundance. Transcription of *fkbp5* was not induced by exposure to PTZ, and basal transcription was GR-dependent (E), whereas PTZ robustly induced transcription of *aplp1*, which was independent of GR function (F) Values are expressed as means +/- s.e.m. A two-way ANOVA identified statistically significant differences in transcript abundance, * p<0.05

Figure 7 – Source data 1. Source data for the analysis of glucocorticoid-induced transcription of *fkbp5* and *aplp1* in wild-type sibling and *stxbp1a*^{sh438} homozygous mutant zebrafish larvae, in the presence or absence of the FKBP5 protein inhibitor SAFit2, as presented in Figures 7A and 7B.

Figure 7 – Source data 2. Source data for the analysis of DNA methylation at the *aplp1* and *fkbp5* GR-DMRs in wild-type sibling and *stxbp1a*^{sh438} homozygous mutant zebrafish larvae, as presented in Figures 7C and 7D.

Figure 7 – Source data 3. Source data for the analysis of *fkbp5* and *aplp1* transcript abundance in wild-type and homozygous *gr*^{s357} mutant larvae maintained in the presence or absence of PTZ, as presented in Figures 7E and 7F.

Figure 8

GR regulates expression of genes encoding metabotropic glutamate receptors in zebrafish.

(A) qRT-PCR analysis of *grm2a, grm2b, grm3 and grm5a* mRNA abundance in the brains of wild-type (GR WT) and homozygous gr^{s357} mutant (GR mutant) adult males. mRNA abundance was normalized to levels of beta actin mRNA, values are displayed as means +/- s.e.m., n = 7. Statistical analysis by *t*-test revealed significantly decreased abundance of *grm2a,* and *grm2b* transcripts, and significantly increased abundance of *grm5a* transcripts, in the brains of *gr*^{s357} mutant compared to wild-type adult males. ** p<0.01, *** p<0.001. Thus, GR promotes co-ordinate expression of *grm2a* and *grm2b* and attenuates expression of *grm5a* in the zebrafish adult brain.

(B) qRT-PCR analysis of *grm2a, grm2b, grm3 and grm5a* mRNA abundance in 5 d.p.f. wild-type and homozygous *gr*^{s357} mutant larvae maintained in E3 medium only (untreated), or E3 medium containing 100μM betamethasone for 2 hours. Histograms show mean mRNA abundance +/- s.e.m., n = 5 pools of 20 larvae per

genotype/treatment group. A two-way ANOVA identified statistically significant differences in transcript abundance: * p<0.05, ** p<0.01, *** p<0.001. Thus, GR is required for glucocorticoid-induced transcription of *grm2a, grm2b, grm3* and for glucocorticoid-mediated inhibition of *grm5a* transcription.

(C) qRT-PCR analysis of *grm2a, grm2b, grm3 and grm5a* mRNA abundance in 4 d.p.f. phenotypically wild-type sibling (*stxbp1a*^{sh438} sibling) and homozygous *stxbp1a*^{sh438} mutant (*stxbp1a*^{sh438} -/-) larvae maintained in E3 medium only (untreated), or E3 medium containing 100μM betamethasone for 2 hours. Histograms show mean mRNA abundance +/- s.e.m., n = 5 pools of 20 larvae per group. A two-way ANOVA identified statistically significant differences in transcript abundance: * p<0.05, ** p<0.01, *** p<0.001. Thus, Stxbp1a is dispensable for glucocorticoid-induced transcription of *grm2a, grm2b, grm3* and essential for glucocorticoid-independent transcription of *grm5a*.

Figure 8 – Source data 1. Source data for the analysis of *grm2a, grm2b, grm3* and *grm5a* transcript abundance in brains of wild-type (GR WT) and homozygous gr^{s357} mutant (GR mutant) adult zebrafish, as presented in Figure 8A.

Figure 8 – Source data 2. Source data for the analysis of *grm2a, grm2b, grm3* and *grm5a* transcript abundance in wild-type (GR WT) and homozygous gr^{s357} mutant (GR mutant) zebrafish larvae maintained in the presence or absence of betamethasone, as presented in Figure 8B.

Figure 8 – Source data 3. Source data for the analysis of *grm2a, grm2b, grm3* and *grm5a* transcript abundance in wild-type sibling (*stxbp1a*^{sh438} sibling) and

homozygous *stxbp1a*^{sh438} mutant (*stxbp1a*^{sh438} -/-) larvae maintained in the presence or absence of betamethasone, as presented in Figure 8B.

Figure 9

Roles for Group I and Group II metabotropic glutamate receptors in regulating synaptic activity-dependent transcription of *aplp1* downstream of GR function. (A,B) qRT-PCR analysis of *aplp1* mRNA abundance in 4 d.p.f. (A) wild-type (GR WT) and *gr*^{s357} homozygous mutant (GR mutant) larvae or (B) sibling and *stxbp1a*^{sh438} mutant larvae. Larvae were first incubated in either DMSO vehicle only, 1μM Group II Grm agonist LY354470, 10μM Grm5a antagonist SIB1893, or the combination of 1μM LY354470 and 10μM SIB1893 for 1 hour. After 1 hour, either ethanol vehicle or betamethasone (from a 10mM stock in ethanol) to a final concentration of 100μM was added, and larvae were incubated for a further 2 hours, after which they were then collected for RNA extraction prior to qRT-PCR analysis. In (A) and (B), histograms show mean *aplp1* transcript abundance for each genotype/treatment group combination +/- s.e.m., relative to that for wild-type larvae incubated in both DMSO and ethanol vehicles; n = 3 pools of 20 larvae per group. A two-way ANOVA identified statistically significant differences in transcript abundance: * p<0.05, ** p<0.01, *** p<0.001

Figure 9 – Source data 1. Source data for the analysis of *aplp1* transcript abundance in (Figure 9 A) wild-type (GR WT) and homozygous gr^{s357} mutant (GR mutant) zebrafish larvae, or (Figure 9B) wild-type sibling (*stxbp1a*^{sh438} sibling) and homozygous *stxbp1a*^{sh438} mutant (*stxbp1a*^{sh438} -/-) larvae maintained in the presence

or absence of betamethasone, and the presence or absence of LY354740 and/or SIB1893.

Figure 10

Identification of potential binding sites for GR in the *fkbp5* promoter and other transcription factors in the *fkbp5* and *aplp1* GR-DMRs.

Binding sites for GR and other transcription factors in the *fkbp5* promoter (top), *fkbp5* GR-DMR (middle), and *aplp1* GR-DMR (bottom), were identified using the JASPAR tool. Three distinct GR binding sites within the fkbp5 promoter are indicated in green, red and blue. CpGs within the *fkbp5* and *aplp1* GR-DMRs are indicated in red.

Figure 11

Schematic overview of the GR-Grm-Stxbp1a-Aplp1 pathway at the synapse

Glucocorticoid-bound GR enters the nuclei of pre-synaptic neurons in the zebrafish larval brain and activates transcription of *fkbp5* and the Group II metabotropic glutamate receptor genes *grm2a, grm2b* and *grm3*, which modulate Stxbp1a-dependent synaptic activity. Glucocorticoid-dependent modulation of synaptic activity then enhances transcription of *aplp1* and attenuates expression of *grm5a* in postsynaptic neurons. Thus, glucocorticoid-dependent activation of the GR-Grm-Stxbp1a-Aplp1 pathway modulates signalling across synapses that could facilitate their adaptive remodeling.

1470 **Figures**
1471

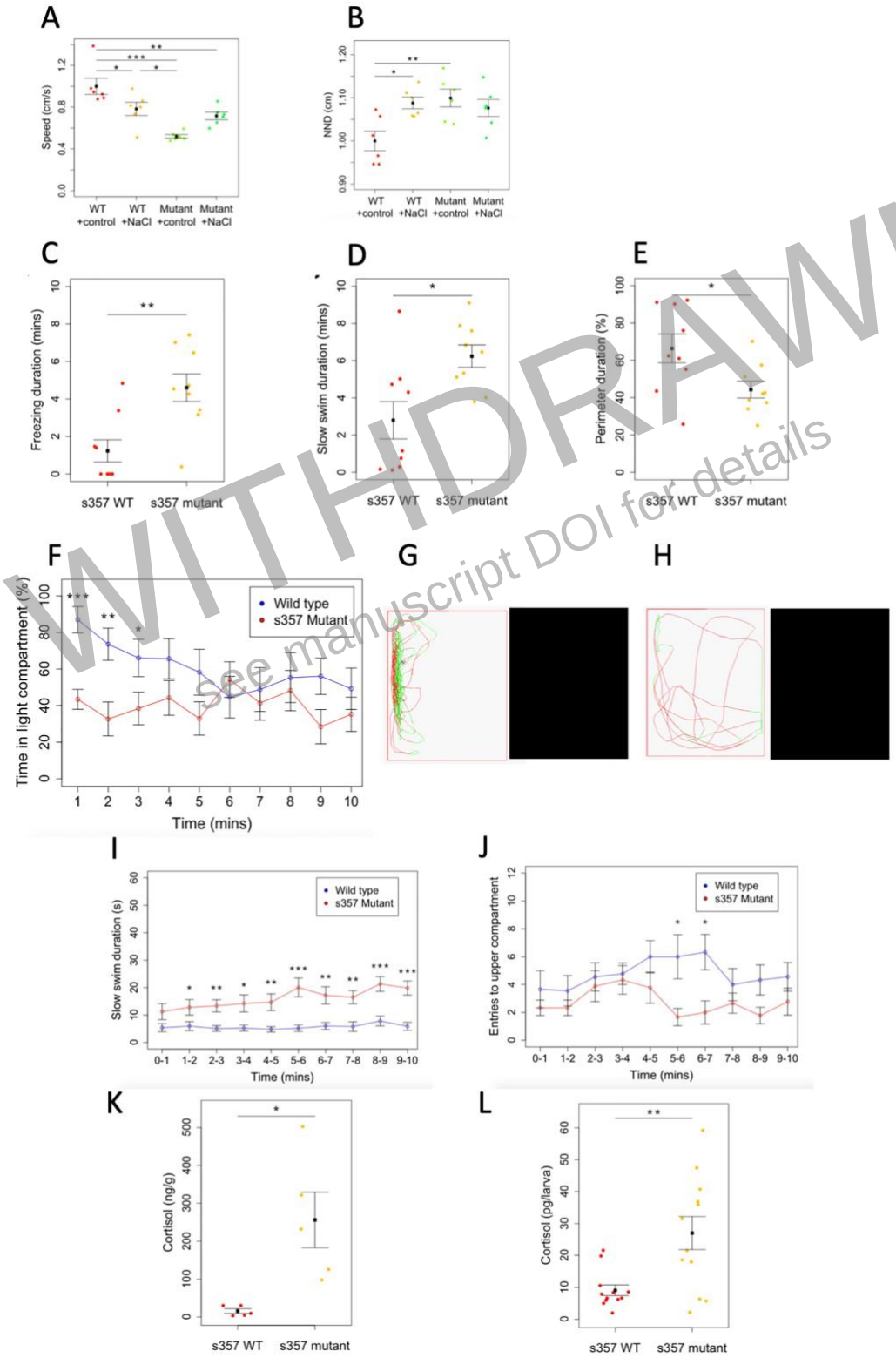

1472

1473 **Figure 1**

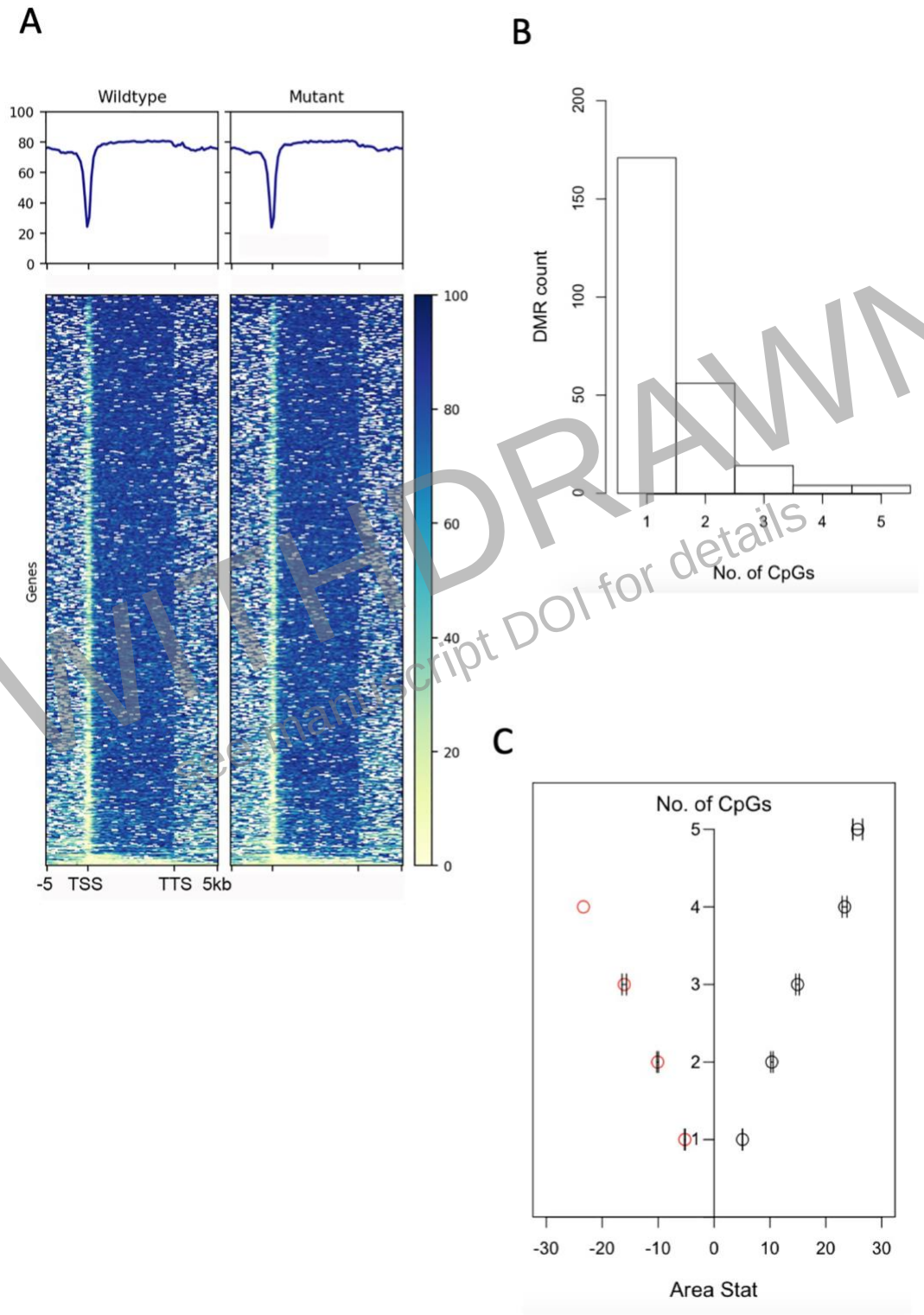

Figure 2

1478

Panther GO Biological Process Term	Number of *Danio rerio* genes	Number of DMR-associated genes	Expected number of genes	Fold-enrichment	+/-	Raw P-value	FDR
mesoderm development	363	10	3.15	3.18	+	1.52E-03	3.28E-02
→ developmental process	1880	37	16.29	2.27	+	3.46E-06	2.74E-04
regulation of catalytic activity	487	13	4.22	3.08	+	4.16E-04	1.23E-02
→ regulation of molecular function	579	13	5.02	2.59	+	1.93E-03	3.51E-02
→ biological regulation	3893	51	33.73	1.51	+	2.48E-03	3.93E-02
cellular protein modification process	928	20	8.04	2.49	+	2.11E-04	7.15E-03
regulation of phosphate metabolic process	656	14	5.68	2.46	+	2.06E-03	3.50E-02
intracellular signal transduction	1498	30	12.98	2.31	+	2.14E-05	1.02E-03
→ signal transduction	2870	51	24.87	2.05	+	6.03E-07	7.14E-05
→ cell communication	3347	58	29.00	2.00	+	2.03E-07	4.82E-05
→ cellular process	9777	116	84.72	1.37	+	2.46E-05	9.71E-04
single-multicellular organism process	1836	30	15.91	1.89	+	9.34E-04	2.46E-02
→ multicellular organism process	1836	30	15.93	1.89	+	9.42E-04	2.23E-02
response to stimulus	3101	43	26.87	1.60	+	1.83E-03	3.61E-02
unclassified	11889	69	103.02	0.67	-	4.03E-06	2.39E-04

1479

1480

1481 **Figure 2 – Figure supplement 1**

1482

1483

Gene annotation	Location	Wild Type	s357 Mutant
fkbp5	6: 41099291- 41099447	2813	3167
npepl1	6: 49743986-49744068	3453	2443
stxbp5l	9: 27628949-27629130	260	432
ptger1c	3: 52284631- 52284792	4065	4908
npy2rl	1: 9551262-9551392	2036	2126
ece2b/lpar6a	15: 4079241-4079376	6447	6498
chrm2a	4: 1213629-1213828	4992	4208
dpp6a	24: 6909239-6909310	3725	4529
gna14	5: 54901068- 54901189	6495	3937
foxred2	3: 25888004-25888127	4101	4397
aplp1	15: 37250007- 37250123	7881	7125

1484

1485

1486 **Figure 2 – Figure supplement 2**

1487

1488

Location	CpG	Gene annotation	p-value	
6: 49743986	1	*npepl1* intron 1	0.0125	*
6: 49743996	2		0.0506	n.s
6: 49744039	3		0.1235	n.s
6: 49744053	4		0.1235	n.s
6: 49744068	5		0.0287	*
6: 41099291	1	*fkbp5* intron 1	0.0003	***
6: 41099385	2		0.1389	n.s
6: 41099420	3		0.0003	***
6: 41099447	4		0.0017	**
15: 37250007	1	*aplp1* intron 1	0.8384	n.s
15: 37250053	2		<0.0001	***
15: 37250055	3		0.00373	**
15: 37250075	4		0.55468	n.s
15: 37250089	5		0.55468	n.s
15: 37250123	6		0.64	n.s

1489

1490

1491 **Figure 2 – Figure supplement 3**

1492

1493

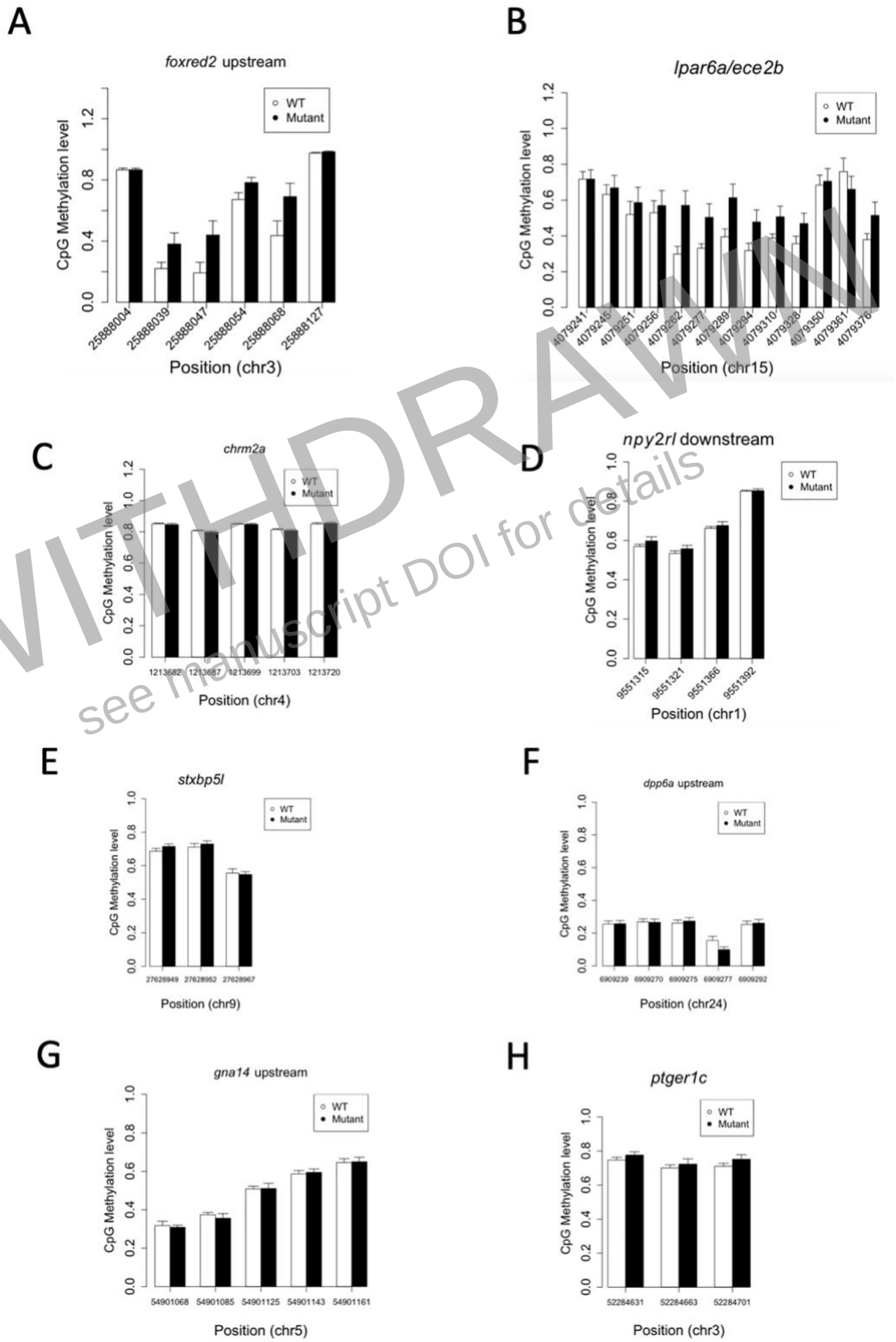

1494

1495

1496 **Figure 2 – Figure supplement 4**

1497

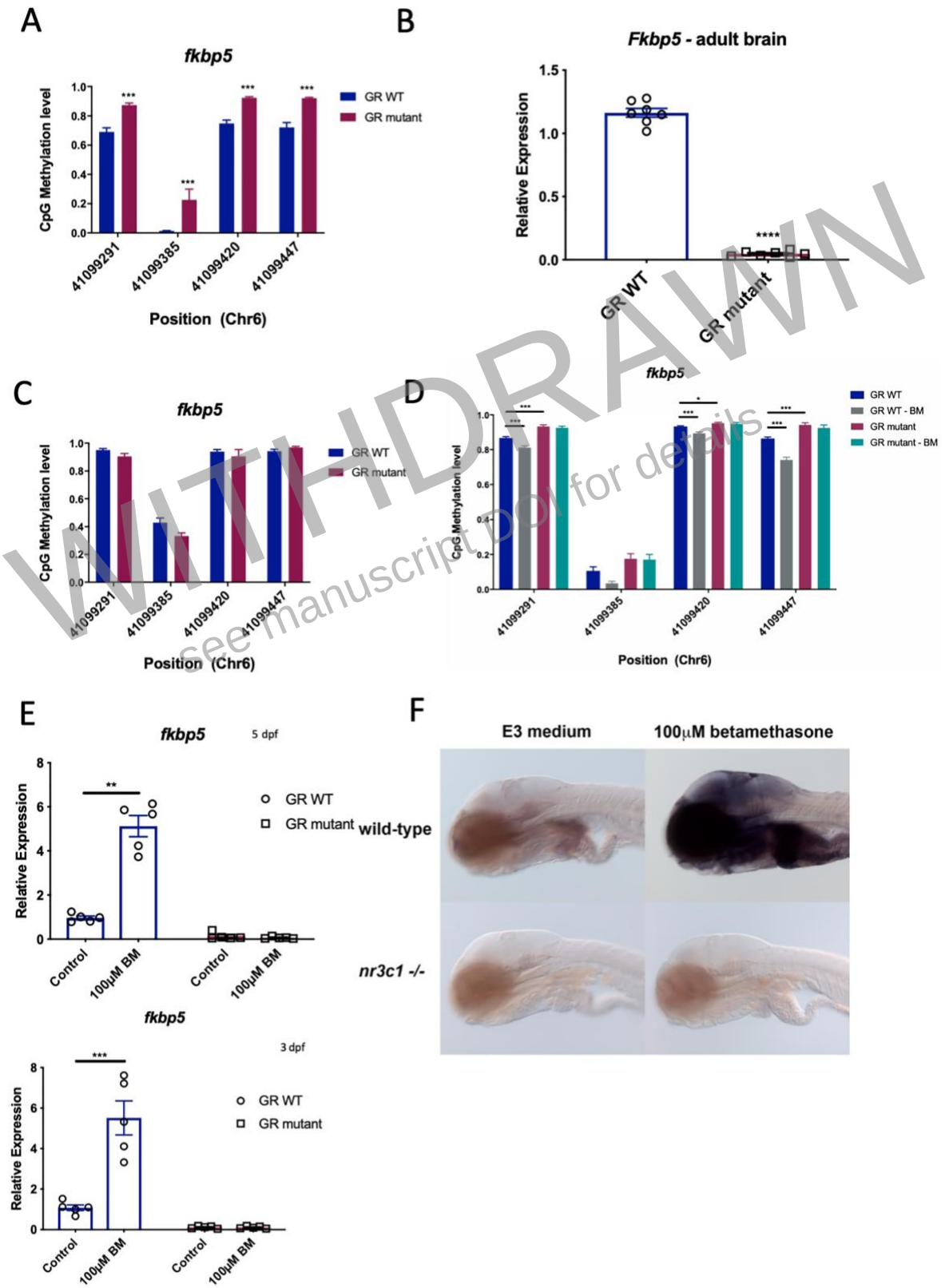

1498

1499 **Figure 3**

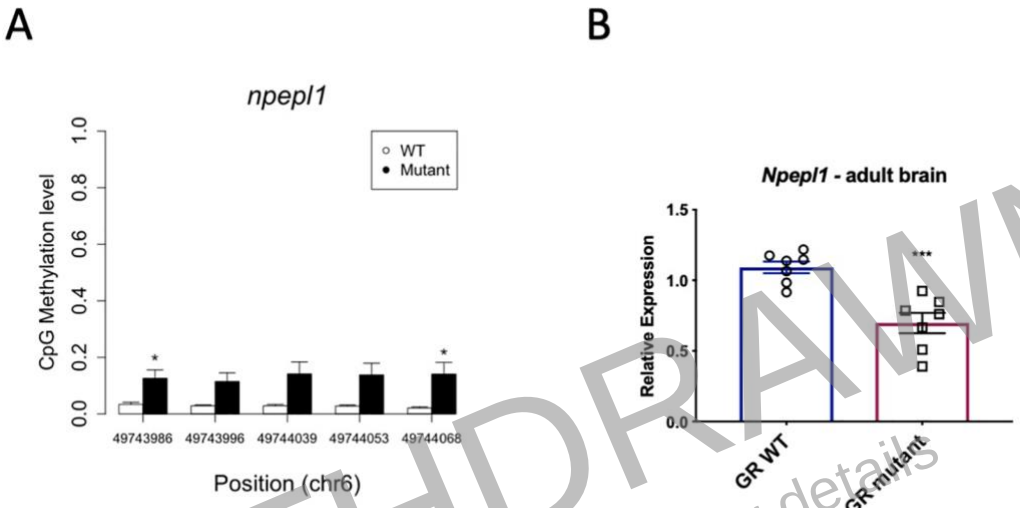

Figure 3 – Figure supplement 1

1508

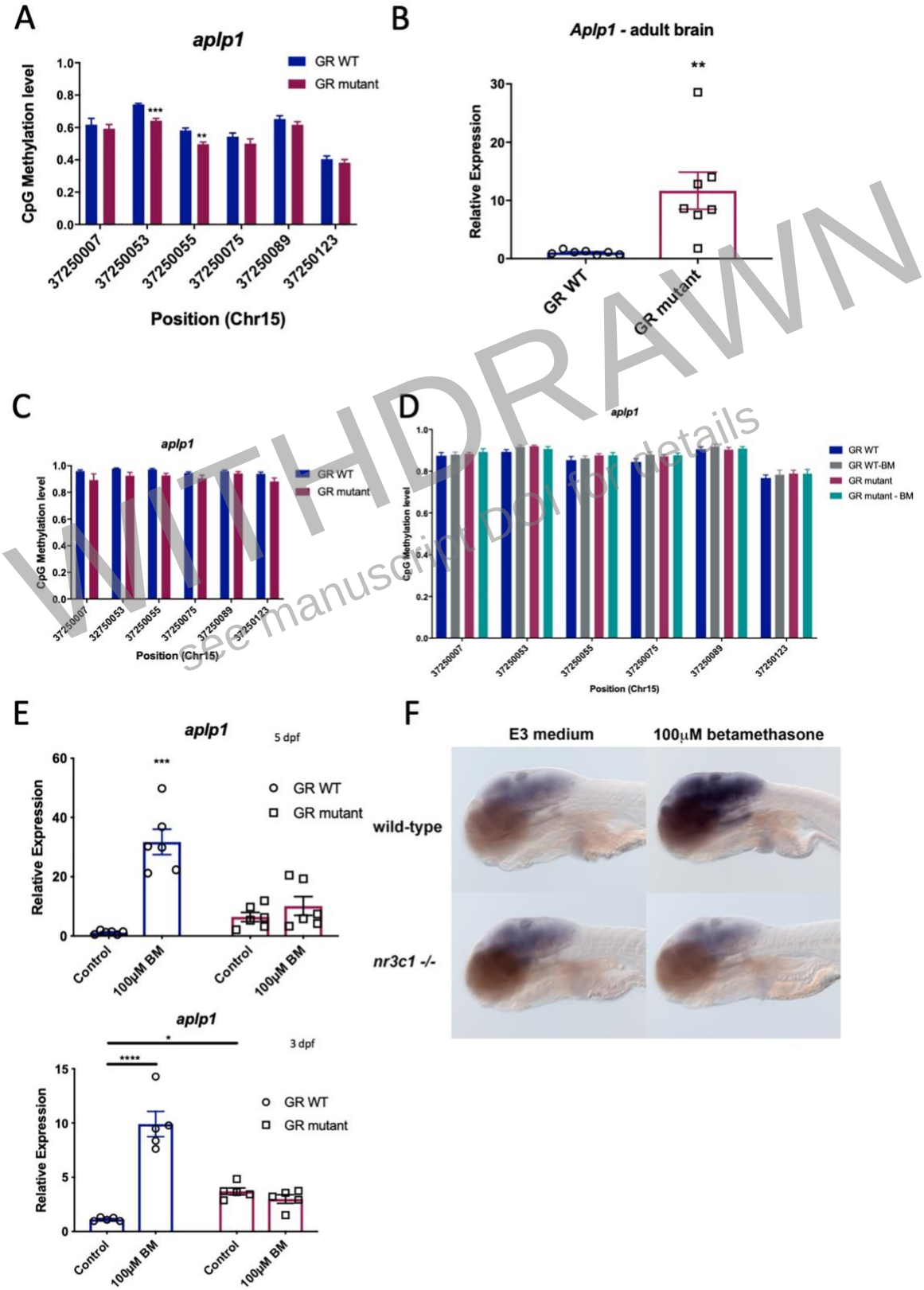

1509

1510 **Figure 4**

1511

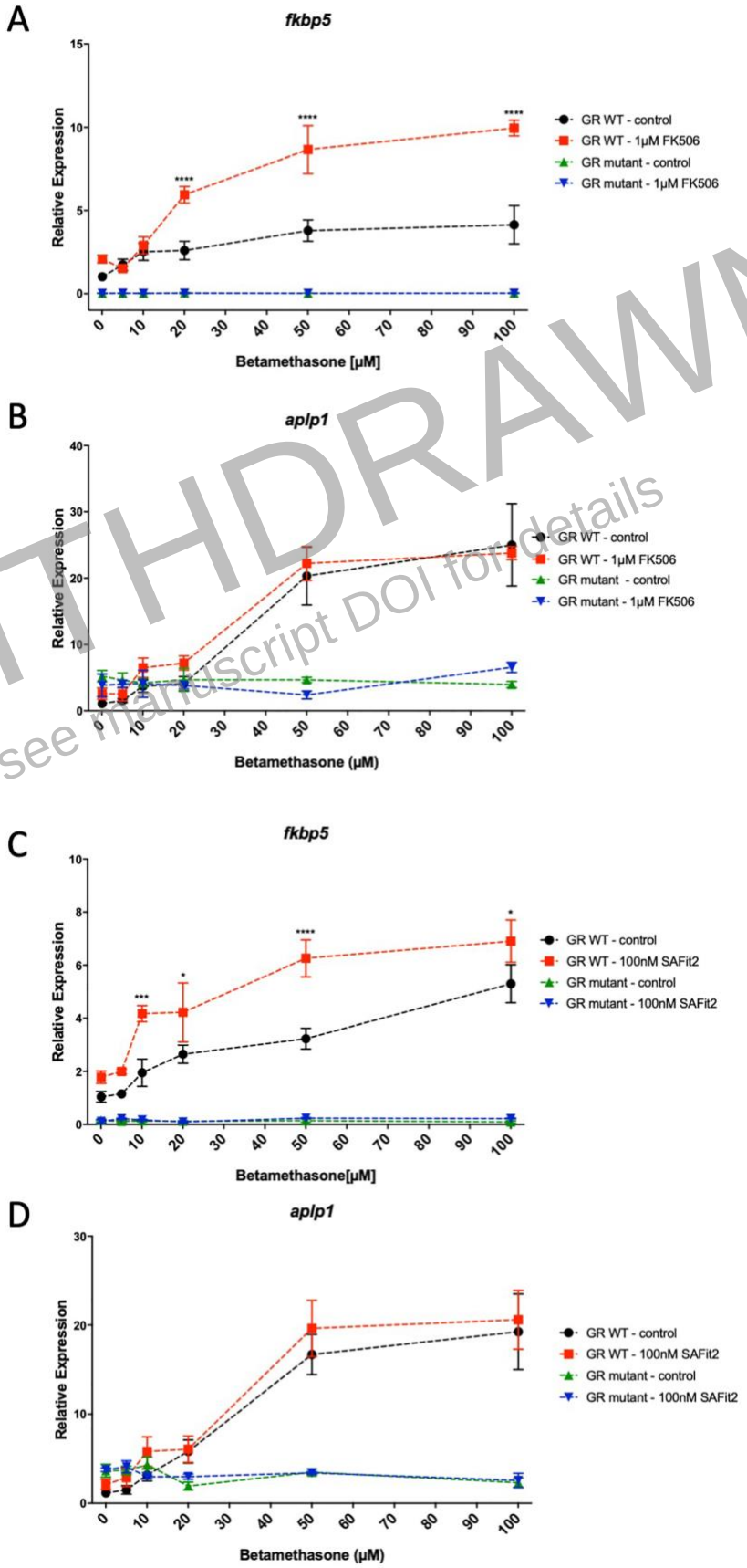

1512

Figure 5

1513

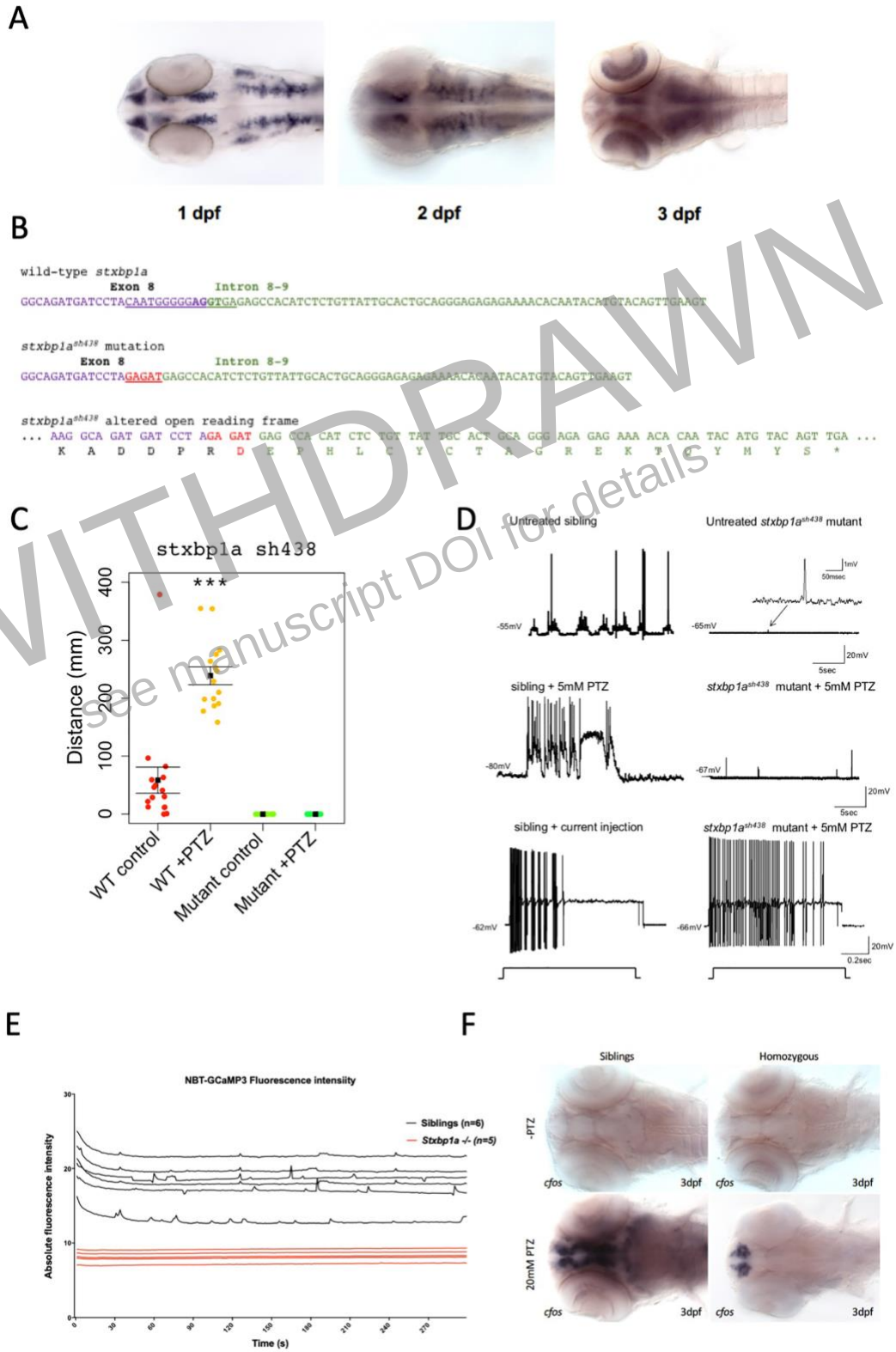

1514

1515 **Figure 6**

1516

1517

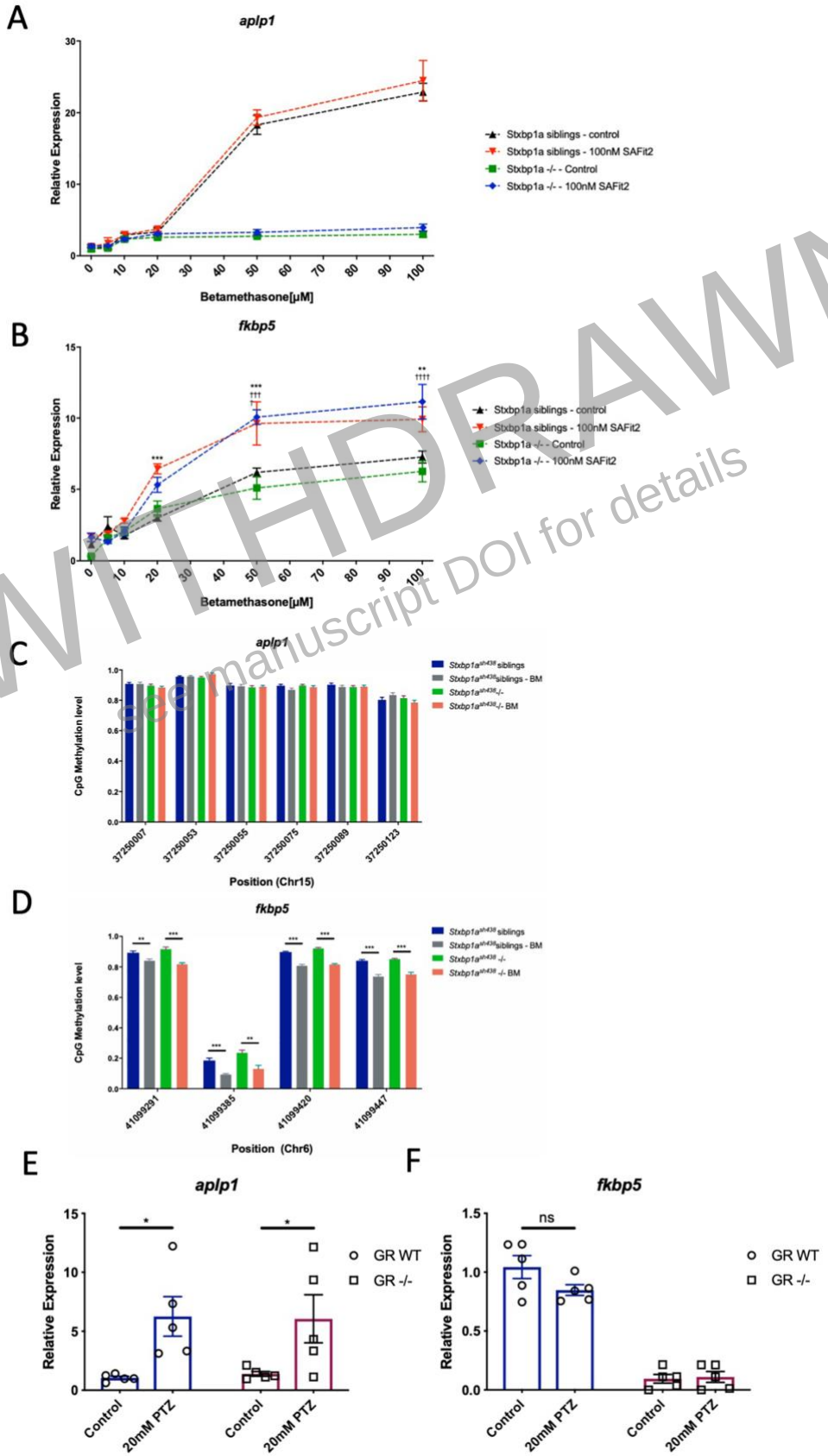

1518

Figure 7

1519

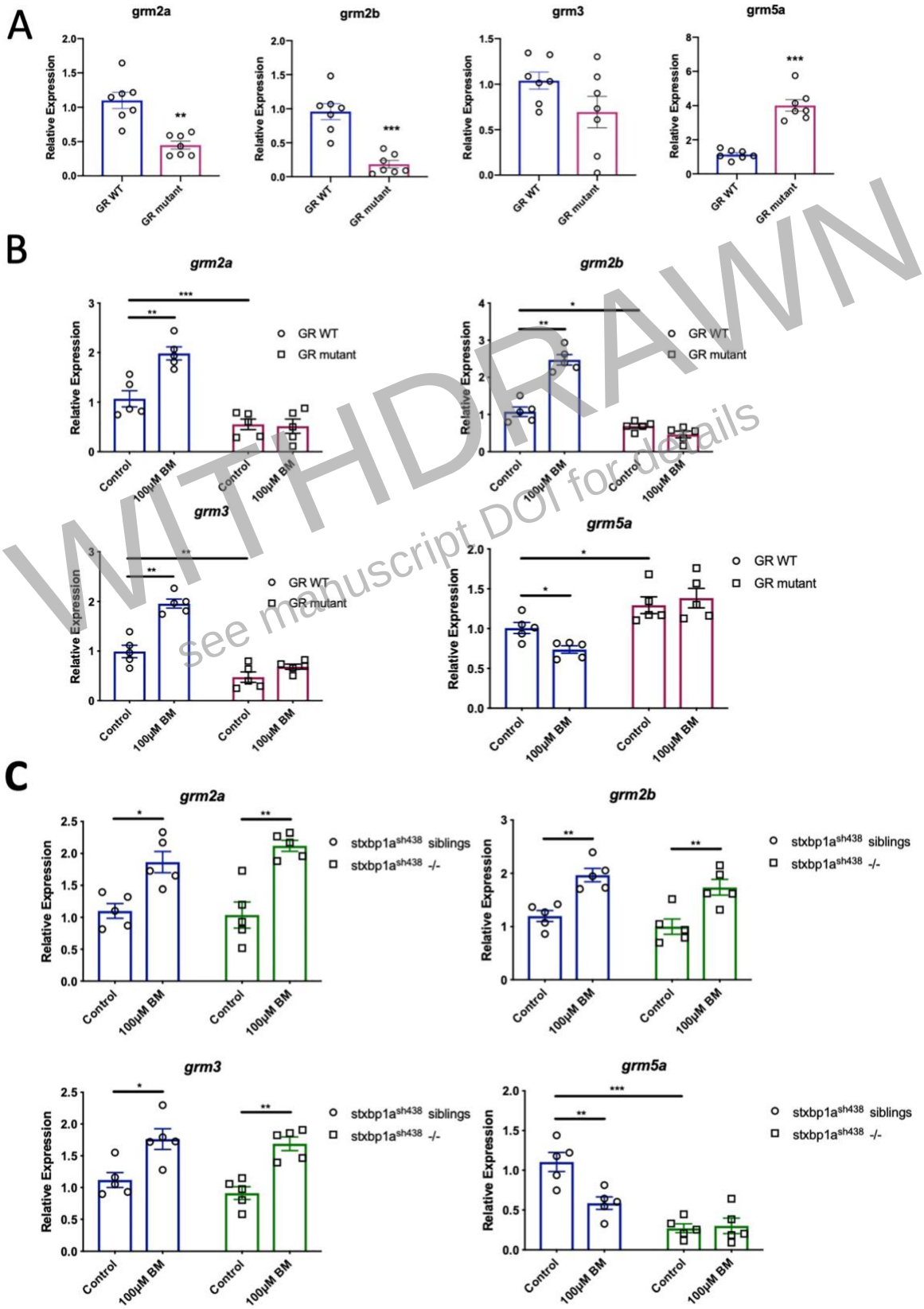

1520

1521 **Figure 8**

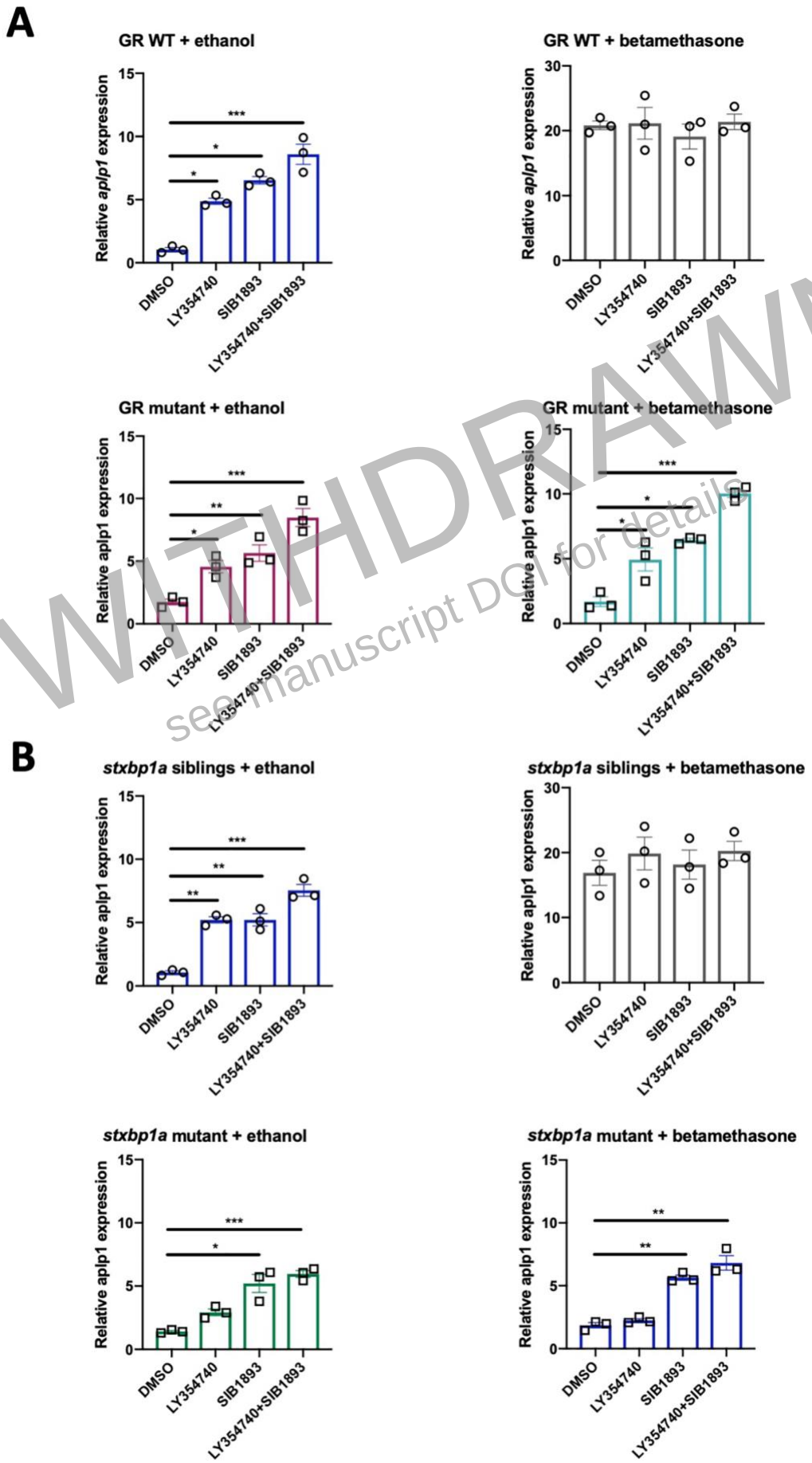

1522

Figure 9

1523

The *fkbp5* promoter contains multiple GREs

AATCATGATGATGATGTTGAATTATATCGCTACACCGGCTCTATTCGATTTTATGCTCAA
TATGCTGCTTTAGTTCTAGGCTTGGTATAGTGTCATCCCGATGGTGTTGTGTGCAGTCTG
TTCTTGCTTTCTGTTTCATCACCTGCATCCTCATCAGAACTGTAAAATATAAACAGCCTA
CCATCCAACACCCACAATCGTCTTCGTAGTATGTTTTTTCTCTACTTATTTTTTTACTTC
CACATTTTTTCTCGACGCAATCTAGTCGTGTTGTTCTTTCCGCGTATCGCTGTGCTCTGT
GTGGTTGTACACGCTGTTCCTAACTTGAGCTGTTCACTCAGCACACAACGGGTTACGGGT
CAGGGTGTCTACTAGGACACTGTGTTCTCATCAGCGCGAGCTACAGTACAGCCGGAACAT
TGTGTTACTTTGTGGACAGTTTCCAAGGCCTGCCCTTAATTTTACTCCACACCGCCCTCC
CCCAGCGTTTACTCCTCCTCCTTTAGTCTCATTTCATTTCCCCCGTCCAAATGTCTCGCA
GAGGCGTATCGTGTTGATGAT
+1

Fkbp5 intron 1

Bold = DMR identified by initial WGBS

Red = CpG

AAAGAGACTGATGTTGTACTGATGGTGTAAAGCCGAGATGTGGTTAAGTGTTTCCTGCCTTTTACTCTTTATTTTGAGATG
TGCTGAGGAGTCAGATGTTTTTATATTTTTATAAATGGTGTCATTTCGTGACCTCAACTAACTGATATCACTGACCAAATTC
GGTTTGAACTTGGTTGCACTGACCTGCGTCTTCAAGCATATTTTCACACTATTTGTTTATA

TF binding sites specific to CpG 1:

Matrix ID	Name	Score	Relative score	Start	End	Strand	Predicted sequence
MA0719.1	RHOXF1	6.4542	0.928687632492	18	25	+	TAAAGCCG

TF binding sites specific to CpG 2:

Matrix ID	Name	Score	Relative score	Start	End	Strand	Predicted sequence
MA0018.3	CREB1	10.2458	0.873101660438	94	105	+	CGTGACCTCAAC
MA0018.3	CREB1	10.2458	0.873101660438	94	105	-	GTTGAGGTCACG
MA0492.1	JUND(var.2)	10.9853	0.910021151889	81	95	-	CGAAATGACACCATT
MA0017.2	NR2F1	10.4685	0.88863282265	92	104	-	TTGAGGTCACGAA
MA0512.1	Rxra	8.57792	0.887886152628	94	104	-	TTGAGGTCACG

TF binding sites specific to CpG 3:

Matrix ID	Name	Score	Relative score	Start	End	Strand	Predicted sequence
MA0068.2	PAX4	8.49127	0.881687643938	123	130	+	CAAATTCG

No strong TF binding sites specific to CpG 4.

Aplp1 intron 1

Bold = DMR identified by initial WGBS

Red = CpGs 2 and 3 found to be hypomethylated in adult GR mutant brains

ATTCATATGTACTTAGAATTTAGTTTTATTATGGGCATTTTAACACTTGTTTGAAAGCAGAAGAGAGCAAAAACTAGTATG
AACGTAAGTGGAAAATGTAAAAAAGCACAAATATTGAAATGAAAAGCACGCGTCAGCTTTGCTCATCAGCCGAAATGG
ATAAATCGCTCTTTAAACATGCACATTAGCCTTCAATGCACGCACCTGCCTGGAAAGAAATGGCAAAATATCATCTTTATCC

TF binding sites specific to CpGs 2 and 3:

Matrix ID	Name	Score	Relative score	Sequence ID	Start	End	Strand	Predicted sequence
MA0006.1	Ahr::Arnt	9.19659	0.982764428382		128	133	-	CGCGTG
MA1099.1	Hes1	10.0756	0.966791899001		126	135	+	AGCACGCGTC
MA0259.1	ARNT::HIF1A	8.5274	0.920298474157		127	134	-	ACGCGTGC
MA0649.1	HEY2	10.2242	0.898251694306		126	135	-	GACGCGTGCT
MA0823.1	HEY1	9.81512	0.891781028421		126	135	+	AGCACGCGTC
MA0104.2	Mycn	10.3227	0.900371094766		126	135	+	AGCACGCGTC
MA0104.1	Mycn	7.79027	0.897764306533		128	133	+	CACGCG
MA0147.1	Myc	10.1463	0.892427955913		126	135	+	AGCACGCGTC
MA0632.1	Tcfl5	7.96715	0.937086785253		126	135	+	AGCACGCGTC
MA0632.1	Tcfl5	7.96715	0.937086785253		126	135	-	GACGCGTGCT

1524

1525 **Figure 10**

1526

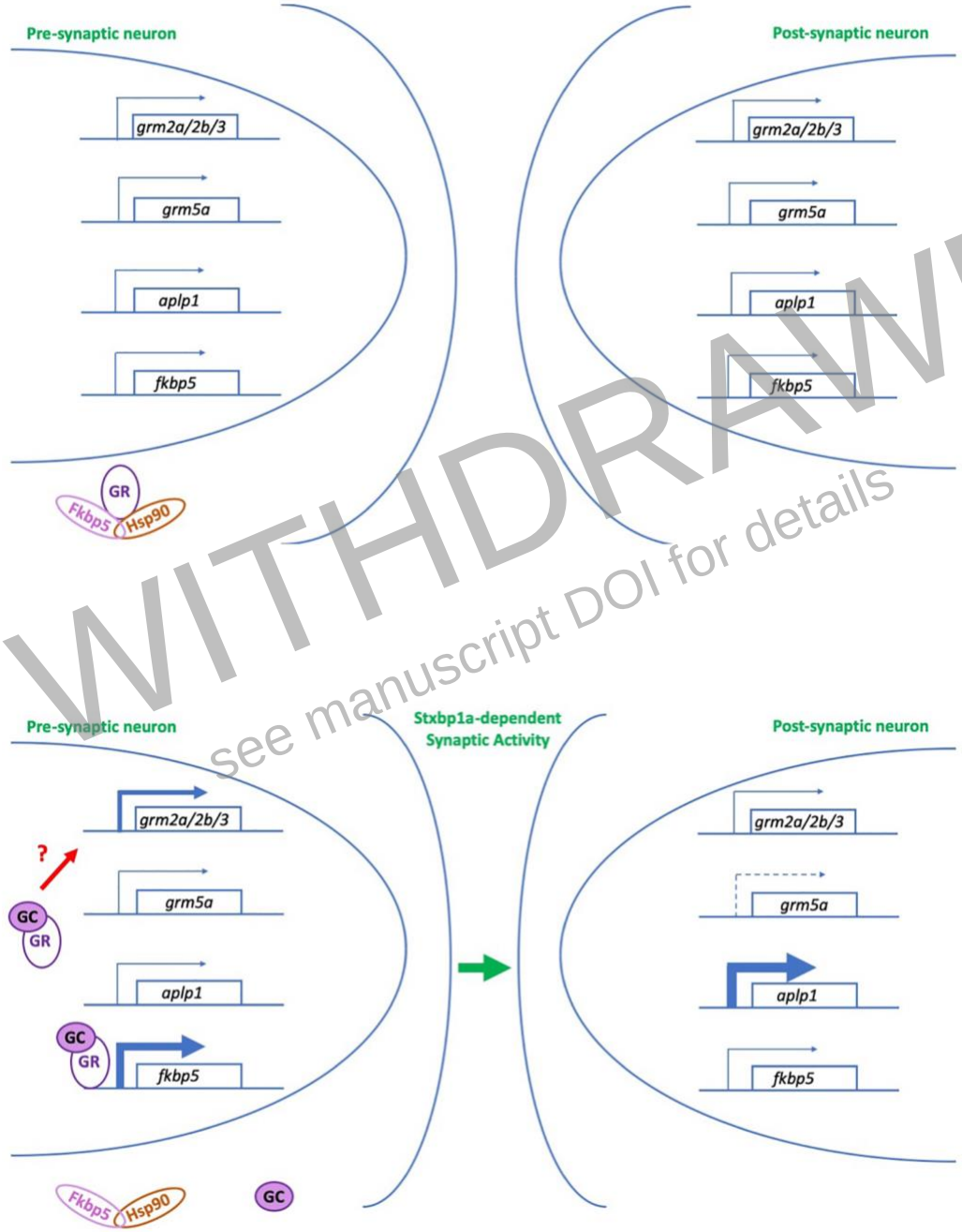

1527

1528

1529 **Figure 11**